

Polymers for Advanced Technologies

As was covered in previous chapters, plastics find important applications for commodity products such as textiles, tires, and packaging. Polymers, particularly thermosets, also find widespread use for composite applications in the automotive, marine, and aerospace industries. Many of these markets have now matured so future growth is expected to be small; however, there are many more applications for polymers that may be less obvious but have great potential and offer challenges for new technologies and growth. Some of these include polymeric membranes for the purification of air and water, for important separations in the chemical and biotech industries, and for proton conduction in fuel cells. Polymers also have important applications in medicine, including uses in controlled drug delivery, artificial organs, and protein synthesis. Some polymers can be made to be electrically conductive and offer potential for the semiconductor industry. Other important specialized applications for polymers include their use as lightweight electrodes and electrolytes for batteries and photovoltaic devices in solar energy conversion. Some newly

developed polymers exhibit unusual optical properties that have attracted significant interest from the defense industries. This chapter seeks to present a picture of these emerging areas in polymer science and engineering.

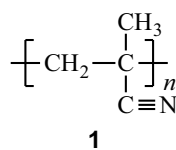
12.1 Membrane Science and Technology

The solubility and diffusivity of gases and liquids in polymers can vary by many orders of magnitude depending upon the chemical structure of the polymer and its conformation, crystallinity, and chain mobility. These differences provide opportunities for the use of polymers in many applications including the separation of gases and liquid mixtures, proton transport through fuel-cell membranes, and food packaging where a barrier is needed against the damaging effects of moisture and/or oxygen.

12.1.1 Barrier Polymers

Good barrier materials for gas and water vapor are important for packaging film, plastic beverage bottles, and the encapsulation of electronic parts (see Section 12.3.6). As an approximate rule of thumb, a polymer with a permeability, or permeability coefficient (P),^{*} less than 10^{-11} cm³-cm/cm²-s cmHg at 0% humidity at 25°C is considered to be a barrier polymer. In general, polymers with high nitrile functionality like polyacrylonitrile (PAN) and the related polymer, polymethacrylonitrile (PMAN, structure 1), have high gas-barrier properties [1]. Because of its attractive CO₂ barrier properties, poly(ethylene terephthalate) is used as the material in the manufacture of plastic bottles for carbonated beverages. As shown by data given in Table 12-1, polyolefins such as polyethylene and polypropylene that are very hydrophobic are good water barriers. Low-density polyethylene film is used as cereal-box liners (O₂ and moisture barrier). Some polar polymers like poly(vinyl alcohol) are very good gas barriers but poor water barriers. Other polymers like poly(vinylidene chloride) (Saran) have both low gas and low water permeability. Polymers that have appreciable water solubility will swell and subsequently exhibit higher gas permeability (i.e., lower gas-barrier properties) when wet than when dry. Salame [2] has proposed a simple group-contribution scheme, the Permachor method, for estimating gas and liquid permeability, particularly for barrier polymers. A review of this approach is included in Chapter 13 (Section 13.1.3).

* Permeability is defined as the amount of a gas passing through a polymer film of unit thickness, per unit area, per second, and at a unit pressure difference.

**Table 12-1 Permeability Coefficients of Selected Polymers at 25°C^a**

Polymer	$P(\text{O}_2)$ ^b	$P(\text{water})$ ^c
Poly(vinyl alcohol)	~0.0001	~5000
Polyacrylonitrile	~0.002	2.45
Poly(vinylidene chloride)	0.012	~0.052
Polymethacrylonitrile	0.012	3.32
Poly(ethylene terephthalate)	0.42	3.2
Poly(vinyl chloride)	0.48	2.5
Poly(vinyl acetate)	3.3	107
Polypropylene	10.8	0.42
Polyethylene (LDPE)	2930.0	0.83
Polyisobutylene	90.0	9.2
Polydimethylsiloxane	~3000	80.5

^a Data taken from ref. [1].^b $P \times 10^{11} \text{ cm}^3\text{-cm/cm}^2\text{-sec cmHg}$ at 0% humidity^c $P \times 10^{11} \text{ g-cm/cm}^2 \text{ sec cmHg}$

12.1.2 Membrane Separations

Although the major uses of membranes are in the production of potable water by reverse osmosis and the separation of industrial gases, membranes can be used for many other important applications. These include the filtration of particulate matter from liquid suspensions, air, and industrial flue gas and the separation of liquid mixtures, such as the dehydration of ethanol azeotropes. More specialized applications include ion separation in electrochemical processes, membrane dialysis of blood and urine, artificial lungs and skin, the controlled release of therapeutic drugs, the affinity separation of biological molecules, membrane-based sensors for gas and ion detection, and membrane reactors. Although membranes can be prepared from metals, ceramics, and microporous carbon and glass, polymeric membranes have great versatility and are widely used. The applications and mechanisms of transport in polymeric membranes are outlined in this section.

Filtration. The most obvious use of membranes is in the filtration of solid particles such as dust, salts, bacteria, and some large viruses from liquids or air streams. As illustrated in Figure 12-1, large organic molecules such as starch and large-diameter bacteria (e.g., *Staphylococcus*) can be filtered by membranes having pore diameters in the range from ca. 1 to 10 μm . Membranes having pore diameters

in the range of 0.01 to 10 μm are called *microfilters*, while those with smaller pore diameters in the range of 10 Å to 1000 Å are called *ultrafilters*. Ultrafilters are suitable for filtering smaller particles, including some bacteria and viruses, as well as some moderately sized organic molecules like sugars. For example, heat-sensitive medical serums can be *cold-sterilized* by microfiltration or ultrafiltration to remove bacterial contamination. Microporous membranes of polypropylene are being evaluated for the removal of SO_2 from flue gas and for the removal of suspended solids and clarification of industrial sewage. Examples of other industrial applications for microfiltration and ultrafiltration are given in Table 12-2.

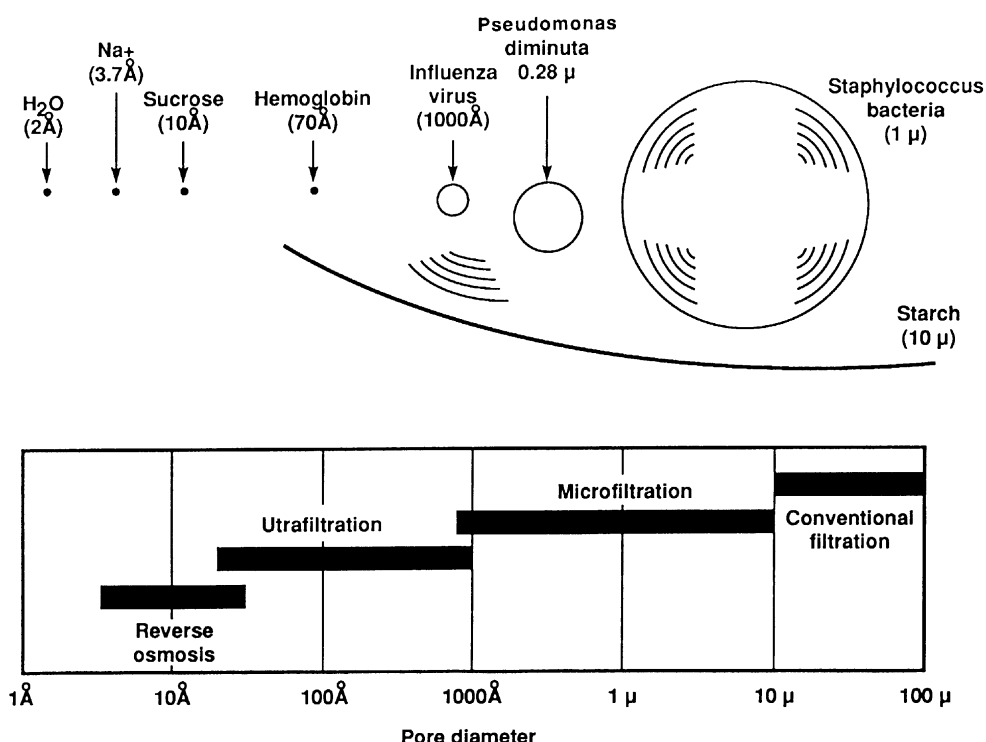


Figure 12-1 Pore sizes and terminology used in filtration. Courtesy of Membrane Technology and Research, Inc., Menlo Park, CA.

Table 12-2 Industrial Applications for Microfiltration and Ultrafiltration Membranes

Industry	Examples
Biotechnology	Product separation from fermentation broth and blood/plasma filtration
Electrocoating	Electrocoat paint filtration
Food	Clarification of apple juice and egg-white concentration
Pharmaceutical	Cold sterilization by removal of microorganisms such as bacteria and yeast cells from aqueous solutions
Semiconductor/electronics	Production of 18 megohm·cm or ultrapure water
Waste management	Oil–water separation and metals recovery

At the extreme limit of filtration is a process called *reverse osmosis* (or hyperfiltration), which is used to obtain potable water from brackish water or salt water. The process is termed “reverse” osmosis since water would be expected to diffuse from the side of low salt concentration to that of high concentration in normal osmosis. In reverse osmosis, a pressure drop up to several thousand psi is used to offset the osmotic pressure differential between fresh and salt water. For successful reverse-osmosis (RO) operation, the diameter of any pores that may be present in the dense separating layer of an RO membrane must be no larger than ca. 5 to 20 Å in order to retain dissolved microsolutes such as salt ions while allowing water to freely transport through the membrane. A polymer frequently used for preparing RO membranes is cellulose triacetate, although some other polymers such as aromatic polyamides and sulfonated polysulfone have been used.

Another growing area in membrane filtration is nanofiltration (NF). The performance of NF membranes falls between that of RO and UF membranes with pore sizes in the area of 10 Å and nominal molecular-weight cutoffs in the range from 100 to 200. Nanofilters are usually prepared as thin-film composite membranes consisting of a thin separating layer containing negatively charged hydrophilic groups attached to a UF-membrane support. Polymers suitable for the separating layer include cellulose acetate, polyamides, poly(vinyl alcohol), and sulfonated polysulfone and polyethersulfone. As illustrated by Figure 12-2, NF membranes retain sugars and some multivalent salts (e.g., $MgSO_4$) but pass many monovalent salts (e.g., $NaCl$) and undissociated acids. Salt rejection is due to electrostatic interactions between ions and the separating layer. Applications for NF membranes include the demineralization of water, the removal of heavy metals, and the removal of lignin and related impurities from wood-pulp streams. Advantages of NF membranes over RO membranes are higher water flux and improved fouling resistance against hydrophobic colloids, proteins, and oils.

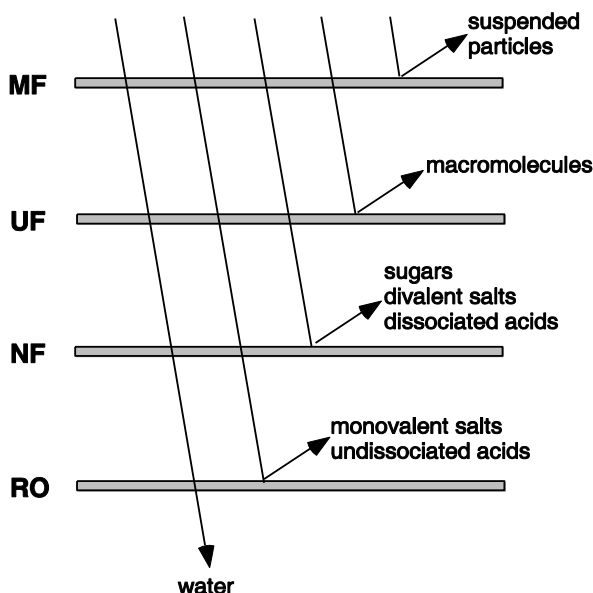


Figure 12-2 Comparison of the rejection performance of microfiltration (MF), ultrafiltration (UF), nanofiltration (NF), and reverse-osmosis (RO) membranes to solutes of different sizes and charge. Adapted from L. P. Raman, M. Cheryan, and N. Rajagopalan, *Chemical Engineering Progress*, March 1994, with permission of the American Institute of Chemical Engineers.

Gas Separations. The potential of using polymeric membranes to separate mixtures of gases may have been realized as early as 1866 when Thomas Graham reported that the oxygen content of atmospheric air could be enriched from 21% to 41% by permeation through a membrane of natural rubber. The first commercial membrane for the large-scale separation of gas mixtures was introduced in 1979. As indicated by Table 12-3, there are several important industrial applications where membrane operations can be competitive with more traditional methods of gas separations, such as cryogenic separation and pressure-swing adsorption (PSA). These include oxygen enrichment of air, hydrogen separation from carbon monoxide and other gases, removal of carbon dioxide from natural gas, and the reduction of organic vapor concentration in air. Other smaller-scale applications include the preservation of food such as apples and bananas during transport by blanketing with low-oxygen-content air, the generation of inert gases for safety purposes, and the dehydration of gases.

Table 12-3 Applications for Polymeric Membranes in Gas Separations

Separations	Suitable Polymers
O ₂ /N ₂	Silicone rubber Polysiloxane- <i>block</i> -polycarbonate Polysulfone Ethylcellulose Poly[(1-trimethylsilyl)-1-propyne] Polypyrrolone Polytriazole Polyaniline
H ₂ from CO, CH ₄ , N ₂	Polysulfone
Acid gases (e.g., CO ₂ and H ₂ S) from hydrocarbons	Cellulose acetate Poly(vinyl chloride) Polysulfone Polyetherimide
Hydrocarbon vapors from air	Silicone rubber

Although ultraporous (i.e., molecular sieve) carbon and certain metallic (e.g., palladium, palladium–silver alloys, and microporous aluminum) as well as ceramic membranes have been used for gas separation, polymers have particularly high selectivity for many important gas mixtures and are easily fabricated into a variety of membrane configurations, such as flat-film, hollow-fiber, and composite membranes consisting of a thin polymer film on a macroporous support. For example, hollow-fiber membranes of polysulfone are used commercially to adjust the H₂/CO ratio in process syn gas for methanol synthesis and the H₂/N₂ ratio in ammonia purge gas.

The selection of a polymer for a particular gas-separation application is guided by the permeability (P_A) and its permselectivity (α_{AB}) for that gas as defined next. The driving force for transport of the gas through the membrane is the pressure drop (Δp) between the high-pressure upside and low-pressure downside of the membrane. Pressure drops may be as high as 2000 psi (13.8 MPa) in certain circumstances.

The *permeability* is defined as the ratio of flux (J_A) to pressure drop as

$$P_A \equiv \frac{J_A \ell}{\Delta p} \quad (12.1)$$

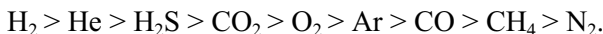
where ℓ is membrane thickness. The most commonly used unit of gas permeability is the barrer that has the value 10⁻¹⁰ cm³ (STP)-cm/(cm²-s-cmHg).

The *permselectivity* of a polymeric membrane for one gas (A) over another gas (B) is given by the ratio of their permeabilities

$$\boxed{\alpha_{AB} = \frac{P_A}{P_B}}. \quad (12.2)$$

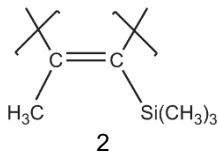
When the permeabilities are measured for pure gases, the permeability ratio is called the *ideal permselectivity*. Since gas mixtures are usually nonideal, especially under high pressure, the actual permselectivity expressed as the ratio of permeabilities for each gas in the mixture may be quite different from the ideal value. Nonetheless, permselectivities are usually reported as ideal values because pure gas permeabilities are more frequently available.

In general, permeability of a polymer for a gas increases with decreasing size and increasing solubility (or condensability) of the gas. The relative permeability of a gas is usually independent of polymer structure and is given in the order of decreasing gas permeability as



As shown by values given in Table 12-4, permeability and, to a lesser extent, permselectivity vary widely with polymer structure and physical state (i.e., rubber, glass, or crystalline).

Generally, permeability is higher while permselectivity is lower for rubbery polymers than for glassy polymers, although a few exceptions exist. An important exception is poly[1-(trimethylsilyl)-1-propyne] (PTMSP, structure 2).



PTMSP is a glassy polymer having higher gas permeability than polysiloxane and almost all other rubbery polymers [3]. This unusually high permeability has been attributed to its high gas diffusivity due to very high free volume. Unfortunately, high free volume leads to an inability of the polymer to differentiate gas molecules on the basis of size and, as a result, permselectivity is low. This inverse relationship between permeability and permselectivity—highly permeable polymers are not selective—is a general one for all polymers [4]. Particularly attractive membrane candidates for a specific gas separation such as O₂/N₂ and CO₂/CH₄ are those polymers whose values of permeability and permselectivity fall near the upper boundary of experimental data as illustrated by the log–log plot of the O₂/N₂ separation factor (α) versus the oxygen permeability separation in Figure 12-3.

**Table 12-4 Gas Permeability and Permselectivity of Representative Polymers
(at 25° to 35°C)**

Polymer	$P(O_2)^a$	$P(O_2)/P(N_2)$	$P(CO_2)^a$	$P(CO_2)/P(CH_4)$
Rubber Polymers				
Butyl rubber	1.3	3.9	5.8	6.6
Natural rubber	24	3.0	134	4.7
Silicone rubber	610	2.2	4553	3.4
Semicrystalline Polymers				
Low-density polyethylene ($\rho = 0.9164$)	2.9	3.0	12.6	4.3
High-density polyethylene ($\rho = 0.964$)	0.4	2.9	1.7	4.4
Poly(ethylene terephthalate) ^b	0.04	4.5	0.30	—
Glassy Polymers				
Cellulose acetate	0.68	3.4	5.5	28
Polysulfone	1.3	5.2	4.9	23
Polycarbonate	1.5	5.2	6.0	23
Polystyrene	2.6	3.3	10.5	—
Poly(2,6-dimethyl-1,4-phenylene oxide)	18	5.0	59	15
Poly(4-methylpentene-1)	29	4.4	93	—
Poly[1-(trimethylsilyl)-1-propyne]	7200	1.7	19,000	4.4

^a Permeability in barrers [$10^{-10} \text{ cm}^3(\text{STP})\text{-cm}/(\text{cm}^2\text{-s}\text{-cmHg})$].

^b $X_c = 0.50$.

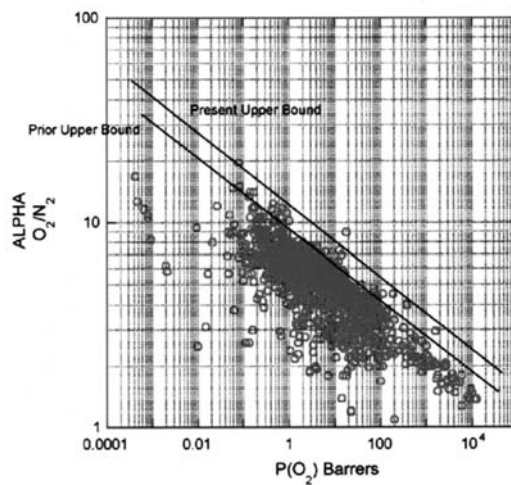


Figure 12-3 Log-log plot of the separation factor for O_2/N_2 versus the permeability coefficient of oxygen. Solid lines represent current and earlier upper boundaries. Reproduced with permission from L. M. Robeson, *The Upper Bound Revisited*. Journal of Membrane Science, 2008. **320**: p. 390–400.

Liquid Separations. Membranes can be used effectively to separate liquid mixtures (e.g., water–organic and organic–organic) in competition with traditional chemical processes such as distillation, adsorption, liquid–liquid extraction, and fractional crystallization. One important membrane operation termed *pervaporation* uses a pressure drop (reduced pressure on the downside) to separate components from a liquid mixture on the basis of preferential solubility and diffusivity in a manner fundamentally similar to gas separation.

In pervaporation, the (liquid) feed mixture is pumped *across* the membrane surface. As illustrated by Figure 12-4, crossflow operation reduces the potential for fouling and concentration polarization by providing a rapid flow at the membrane surface to sweep away contaminating particles and to encourage mixing at the membrane–liquid interface.

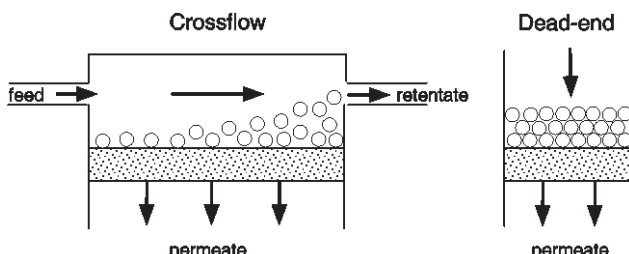


Figure 12-4 Illustration of a crossflow membrane process (left) compared to dead-end filtration (right).

A representative process flow chart for pervaporation is illustrated in Figure 12-5. Vacuum (i.e., vacuum pervaporation) or reduced pressure (i.e., sweep-gas pervaporation) is applied at the downside of the membrane. Separation occurs by selective solution diffusion (see Section 12.1.3) and subsequent evaporation at the downside and is driven by the partial-pressure gradient between the liquid feed and the permeate vapor. The permeate vapor phase is condensed and recovered as the product stream. The portion of the feed that is not permeated is called the *retentate*.

Related processes include *pertraction*, by which the permeate is dissolved in a circulating carrier fluid rather than being vaporized, and vapor permeation or *evapomeation*, where the feed stream is a vapor or vapor–gas mixture and, therefore, no phase change occurs during the process. In general, pervaporation can be used to separate structural isomers, to separate components from azeotropic and close boiling mixtures, to recover trace substances, and to displace the equilibrium of a chemical reaction. Commercial uses of pervaporation include the concentration of ethanol produced by the fermentation of biomass (e.g., starch, sugar, and cellulose), the removal of trace organic compounds from water supplies, and the separation of mixtures of organic compounds. Vapor permeation (i.e., evapomeation) may be used to remove trace organic compounds from air or in hybrid distillation processes.

whereby a separate membrane stage may be used in addition to more traditional distillation processes. The choice between pervaporation and other separation processes such as distillation is largely controlled by economics. In pervaporation, the principal form of energy utilization is the heat of vaporization of the permeate. Economics are particularly favorable for pervaporation in the case of the separation of azeotropic mixtures such as ethanol and water.

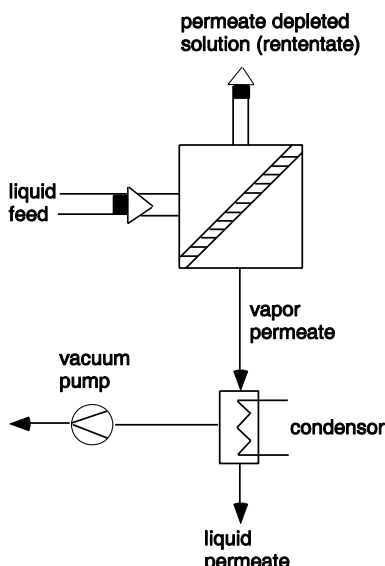


Figure 12-5 Schematic of membrane-pervaporation process. A binary liquid mixture passes crossflow over a polymeric membrane and the permeate, enriched in the more permeable component, is vaporized on the downside (low-pressure side), condensed, and collected. Courtesy of Membrane Technology and Research, Inc., Menlo Park, CA.

Membranes for pervaporation may be dense (homogeneous) membranes, asymmetric membranes, or composite membranes consisting of a thin permselective polymeric layer covering a microporous support. For alcohol–water separation, cellulose derivatives provide high permeability with moderate selectivity. Poly(vinyl alcohol) (PVA), used as a graft copolymer or as the separating layer in a composite membrane, has preferential permeability to water over alcohols or other organic molecules, while silicone rubber is more permeable to alcohols (also aldehydes and ketones) than to water.

Flux in pervaporation is a function of a diffusion term (D_o), the concentration of the penetrant (C_i), and the strength of penetrant-membrane (polymer) interaction (γ) and is inversely dependent on membrane thickness (ℓ) as

$$J_i = \frac{D_o}{\gamma \ell} [\exp(\gamma C_i) - 1]. \quad (12.3)$$

The selectivity for component A over B in a binary liquid mixture may be expressed by the *separation factor* (α_{AB})

$$\alpha_{AB} = \frac{y_A / y_B}{x_A / x_B} \quad (12.4)$$

or by the *enrichment factor* (β_A), the ratio of concentrations (typically in mass units) of the preferentially pervaporating species (A) in the permeate and feed

$$\beta_A = \frac{y_A}{x_A} \quad (12.5)$$

where x_A and y_A represent the concentration in the feed (i.e., liquid phase) and permeate (i.e., vapor phase), respectively.

Other Separations. In addition to the major membrane processes—filtration, gas separation, and pervaporation—several other fundamental membrane operations are important to the chemical and biomedical industries, such as those listed in Table 12-5. Processes like electrodialysis that can be used to desalt ionic solution use ion-exchange membranes, which are swollen gels or microporous membranes carrying a fixed positive or negative charge. For example, anion-exchange membranes have fixed positive charges (typical charge density of 2 to 4 milliequivalents per gram of membrane) that bind anions from solution. Separation is based upon exclusion of co-ions (same charge as fixed ions of the membrane).

An important application for membranes is in electrochemical processes such as the production of caustic, as shown in Figure 12-6. In this process, water enters at the cathode compartment while saturated brine (NaCl) is fed to the anode compartment. Electrodes are separated by a perfluorosulfonate ionomer membrane such as Nafion (see Section 10.2.4), which has a low diffusion coefficient for Cl^- and a high diffusion coefficient for Na^+ . Water is decomposed at the cathode to produce concentrated sodium hydroxide and hydrogen. At the anode, chloride ions are reduced to chlorine, while the sodium ions are able to permeate the membrane to the cathode compartment, and the anions (Cl^- and OH^-) are excluded. The mechanism of transport through perfluorosulfonate ionomer membranes is briefly discussed in Section 12.1.3.

Table 12-5 Other Membrane Processes

Process	Applications	Driving Force	Membrane Type	Applications
Dialysis	Separation of colloids and other large particles from inorganic ions and other small particles	Concentration gradient	Hydrophilic ultrafilters	Artificial kidney Plasma purification; caustic recovery in the viscose process
Electrodialysis	Separation of ions having opposite charges	Electrical potential	Ion exchange	Concentration of electrolyte solutions; desalting
Electro-osmosis	Treatment of colloidal suspensions and sludge in effluent and waste streams	Electrical potential	Ion exchange	Dewatering

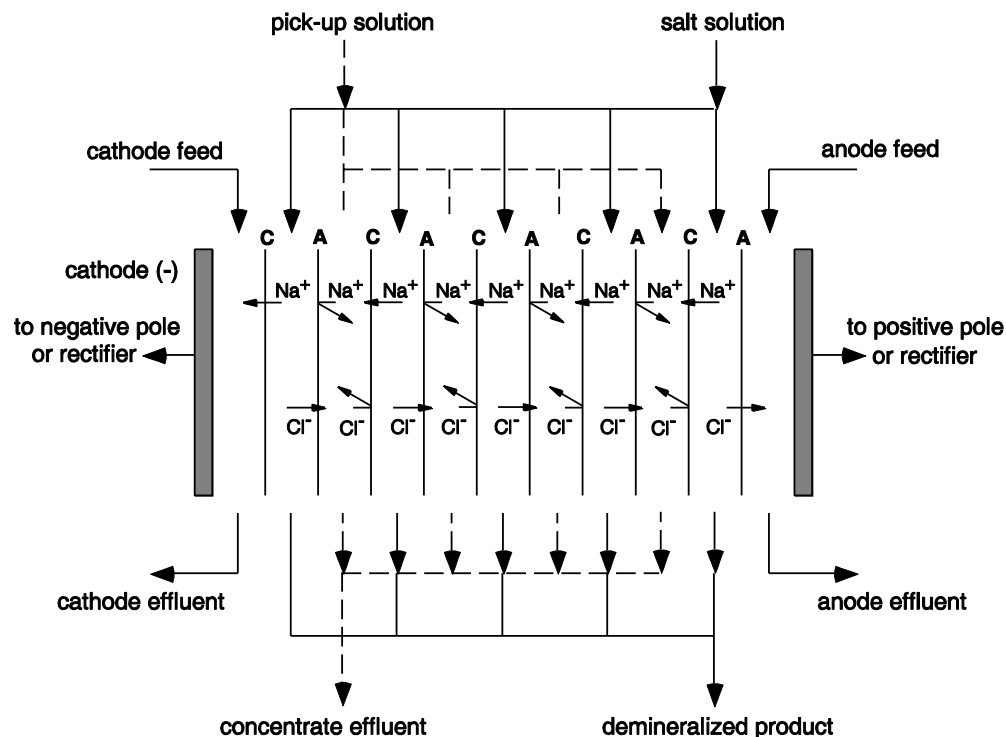


Figure 12-6 Typical chlor-alkali cell used in the production of caustic. Courtesy of Membrane Technology and Research, Inc., Menlo Park, CA.

Fuel Cells. Polymeric membranes also have important potential in the development of efficient and inexpensive fuel cells that could be used to power electric cars and have other important aerospace and military applications. An illustration of a proton-exchange fuel cell is shown in Figure 12-7. At the anode, hydrogen is ionized. Electrons produced by the ionization travel through the external circuit (i.e., the electric motor) and return to the cathode, where they combine with oxygen to form oxygen ions. These reactions are accelerated by the platinum catalyst. The hydrogen ions (i.e., protons) travel through a polymer membrane to the cathode, where they combine with the oxygen ions to form water. As in the case of the chlor-alkali process, perfluorosulfonate ionomers such as Nafion are effective membrane polymers for fuel-cell applications. In addition to the use of hydrogen for fuel cells, natural gas, hydrocarbons, and methanol may be used as fuel. In the case of direct methanol fuel-cell applications, an aqueous methanol solution is delivered to the anode (air to the cathode). Carbon dioxide and water are by-products. A problem in the selection of a fuel cell membrane has been methanol crossover (diffusion from the anode to the cathode) [5], which is a particular problem for Nafion through which methanol easily diffuses. In this case, a variety of sulfonated polymers including some polyphosphazenes (see Section 10.2.5) show promise.

12.1.3 Mechanisms of Transport

The two principal modes of transport that can occur in membrane separations are *size exclusion* in the case of porous membranes and *solution diffusion* in the case of nonporous or dense membranes. Size exclusion is determined by the diameter of the pore in relation to the penetrant size and diffusional path (i.e., mean free path in the case of gases). Size exclusion may be used to separate particles as large as $10 \mu\text{m}$ or as small as a couple of angstroms in the case of gas molecules. The size and (Lennard-Jones)* collision parameters for several industrially important gas molecules are given in Table 12-6.

* The potential energy, U , is the work required to bring two gas molecules from infinite distance to some separation distance, r , as illustrated:

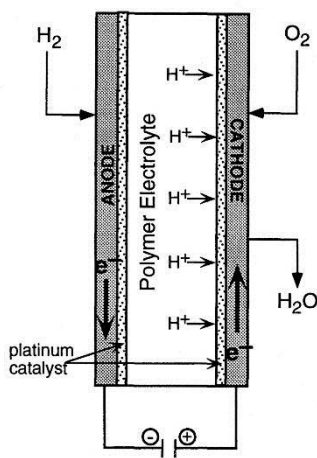
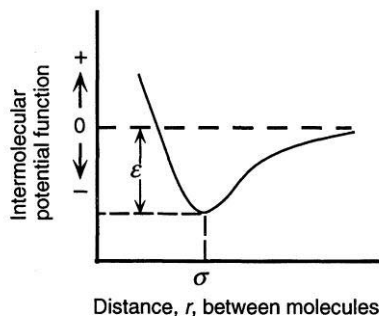


Figure 12-7 Illustration of a typical fuel-cell configuration.



The Lennard-Jones or 6–12 potential function is given as

$$U = 4U = 4\varepsilon \left[\left(\frac{\sigma}{r} \right)^{12} - \left(\frac{\sigma}{r} \right)^6 \right]$$

where ε is the depth of the potential well and σ is the distance of separation at which the potential energy reaches a minimum.

Table 12-6 Kinetic Diameters and Lennard-Jones Potential Well Depth^a of Important Gases

Gas:	He	H ₂	CO ₂	O ₂	N ₂	CO	CH ₄
Kinetic diameter (Å)	2.6	2.89	3.3	3.46	3.64	3.76	3.80
ε/k (K)	10.2	59.7	195	107	71.4	91.7	149
σ (Å)	2.55	2.83	3.94	3.47	3.80	3.69	3.76

^aSee text footnote for identification of the Lennard-Jones parameters ε/k and σ .

Transport through nonporous membranes is controlled by the solubility and diffusivity of the penetrant in the polymer matrix. In this regard, the transport of gases through a glassy polymer differs from that in a rubbery polymer. This is a result of an additional mode of sorption that is available in glassy polymers—the filling of Langmuir-type microvoids or regions of localized high free volume present in the glassy state. A discussion of diffusion through porous media and the solution-diffusion model is presented in the following sections, as are two other more specialized membrane-transport processes—facilitated and coupled transport and transport through perfluorosulfonate ionomers.

Transport through Porous Media. As illustrated in Figure 12-8, the mechanism of flow of gas molecules through porous membranes depends upon the size of the pores in relation to the *mean free path* of the gas molecules. The mean free path represents the average distance traversed by gas molecules between collisions. The Knudsen number (N_{Kn}) is defined as the ratio of the mean free path to the mean pore diameter. When the Knudsen number is small, flow is inversely proportional to the viscosity of the fluid (gas). This is called *viscous flow*, illustrated in Figure 12-8A. In contrast, *Knudsen flow* occurs when the Knudsen number is large (i.e., for small pore sizes). In this case, molecules diffusing within the pores collide much more frequently with the pore walls than with themselves (Figure 12-8B). The Knudsen diffusion coefficient is inversely proportional to the *square root* of the molecular mass (M) of the diffusing species following the relationship

$$D_{Kn} = \frac{d}{3} \left(\frac{2RT}{M} \right)^{1/2} \quad (12.6)$$

where d is the pore diameter. Although some separation can be achieved by selective Knudsen flow of gas molecules, permselectivity is small unless the molecules are very different in size. A third mechanism occurs when the pore diameter is small compared to the molecular diameters of the diffusing molecules. This is termed *molecular sieving* (Figure 12-8C). Small molecules can also diffuse through dense molecules (Figure 12-8D) through a solution-diffusion mechanism discussed in the following section.

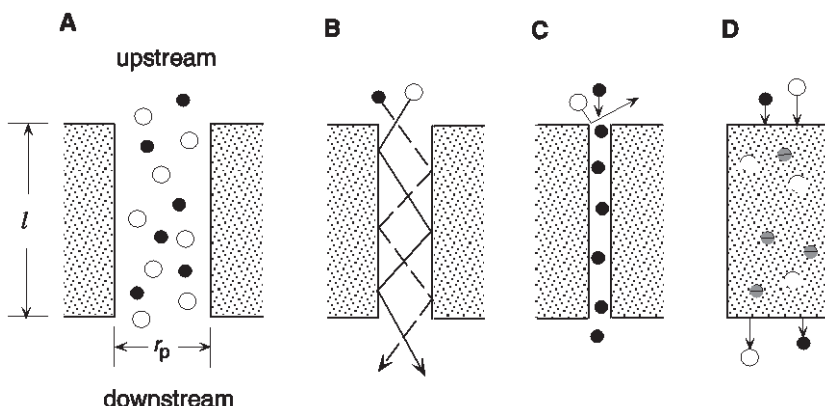


Figure 12-8 Illustration of the membrane transport of two differently sized molecules by various mechanisms. From left to right: (A) viscous flow through large pores of radii r_p (no separation); (B) Knudsen flow (separation based upon difference in molecular weights); (C) molecular sieving (separation due to relative diffusive rates and surface sorption on pore walls); and (D) solution–diffusion transport through a dense membrane (separation based upon relative solubility and diffusivity).

Solution-Diffusion Transport. The predominant mechanism of transport for industrial gas- and liquid-separating membranes involves the dissolution and subsequent diffusion of molecules in a nonporous or dense membrane. In general, the permeability can be represented as the product of the solubility, S , and diffusivity, D , coefficients of the penetrant in the polymer membrane as

$$\boxed{P = SD} \quad (12.7)$$

The mechanism of penetrant *solubility* in a polymeric membrane depends upon the activity of the penetrant and whether the polymer is in the rubbery or glassy state. The solubility of organic vapors at very low activities and gases at low to moderate pressures in liquids and rubbery polymers is given by *Henry's law* expressed as

$$\boxed{C = Sp} \quad (12.8)$$

where C is the concentration of sorbed penetrant (typically units of cc of gas at STP per cc of polymer) and p is the pressure. In general, the solubility of a gas increases with its condensability. More condensable gases are those with higher boiling points or critical temperatures, such as CO_2 . At higher penetrant activities, as is the case for organic vapors and highly condensable gases like CO_2 at moderate to high pressures, Henry's law no longer applies. In this case, the Flory–Huggins lattice model (see Section 3.2.1) may be used to represent the observed increase in solubility with

increasing pressure in rubbery polymers (i.e., $T > T_g$). An illustration of this behavior is shown in Figure 12-9, which plots the sorbed concentration of CO_2 in a silicone elastomer against pressure. Below approximately 400 psia, sorption is adequately represented by the linear relationship given by Henry's law. At higher pressures, the sorbed concentration increases at an increasing rate as modeled by the Flory–Huggins theory.

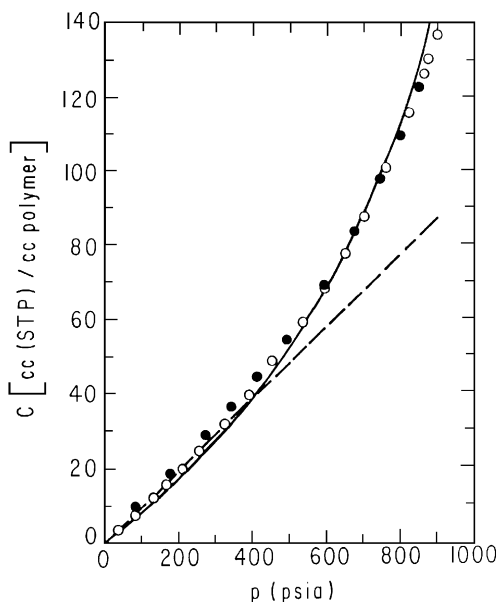


Figure 12-9 Sorption isotherm of CO_2 in silicone rubber at 35°C . Data points give CO_2 concentrations measured at different pressures during sorption (\circ) and desorption (\bullet). The solid line represents the fit by the Flory–Huggins equation; the broken line represents Henry's law behavior. Reprinted with permission from G. K. Fleming and W. J. Koros, *Macromolecules*, 1986, **19**: p. 2285. Copyright 1986, American Chemical Society.

Below T_g and at low to moderate gas pressures, the sorption isotherm curves downward with increasing pressure, as illustrated by the data for polysulfone in Figure 12-10. The most successful model for sorption in glassy polymers is given by the *dual-mode* model [6], which postulates that an additional (Langmuir) mode of sorption is possible by the filling of microvoids in the glassy state. The total sorbed concentration is then a summation of Henry's law dissolution (C_D) and Langmuir-type hole-filling (C_H) contributions as

$$C = C_D + C_H = k_D p + \frac{C'_H bp}{1 + bp} . \quad (12.9)$$

The parameters characterizing dual-mode sorption are the Henry's law coefficient, k_D , the Langmuir or hole-filling capacity of the glass, C'_H , and the hole-affinity parameter, b . Dual-mode parameters for representative polymers are given in Table 12-7.

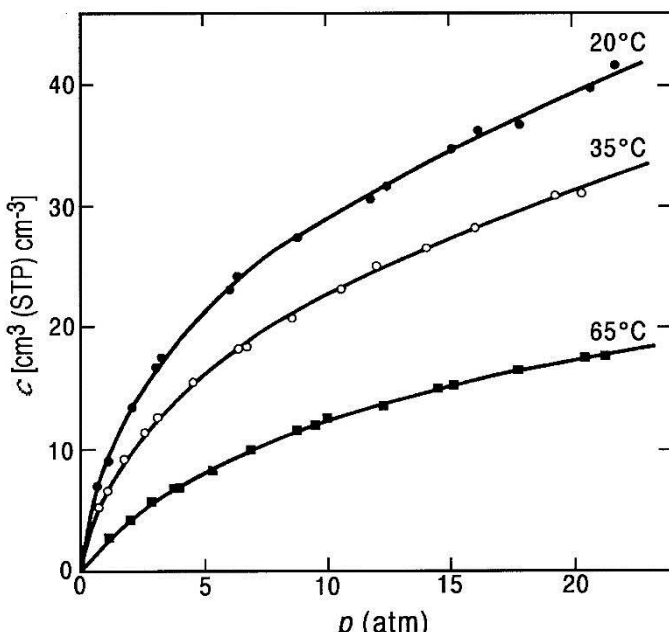


Figure 12-10 Sorption isotherm of CO_2 in a glassy polymer, polysulfone ($T_g = 186^\circ\text{C}$), showing dual-mode behavior. As temperature is decreased from 65°C to 20°C , the isotherm becomes increasingly nonlinear as the Langmuir capacity increases with increasing $T - T_g$. Adapted from Y. Maeda and D. R. Paul, *Effect of Antiplasticization on Gas Sorption and Transport. I. Polysulfone*. Journal of Polymer Science: Part B: Polymer Physics, 1987. **25**(5): p. 957. Copyright © 1987 John Wiley & Sons. Reprinted by permission of John Wiley & Sons, Inc.

As discussed earlier, the Henry's law coefficient, k_D , is strongly influenced by the condensability of the gas. For example, k_D is especially high for CO_2 (see Table 12-7), which is a very condensable gas. In turn, the condensability of a gas can be related to ε/k , the well depth of the Lennard-Jones potential-energy plot for a gas.

Values of ε/k were given for some gases in Table 12-6. For a given polymer, k_D is exponentially related to ε/k as [7]

$$\ln k_D = \ln k_D^0 + m \frac{\varepsilon}{k} \quad (12.10)$$

where k_D^0 is a constant for a given polymer and temperature and m is the slope ($\sim 0.01 \text{ K}^{-1}$) of a plot of $\ln k_D$ versus ε/k . The second contribution to solubility for glassy polymers—the Langmuir capacity, C_H' —depends upon the size and distribution of microvoids and, therefore, can be related to the free volume of the glass. Free volume is determined by the stiffness and molecular dimensions of the polymer chain and the extent of undercooling of the glass.

Table 12-7 Representative Dual-Mode Parameters for Sorption of Nitrogen, Methane, and Carbon Dioxide in Important Gas-Separating Polymers at 35°C

Polymer	k_D ($\text{cm}^3(\text{STP})/\text{cm}^3$ -atm)	C_H' ($\text{cm}^3(\text{STP})/\text{cm}^3$)	b (atm^{-1})
Cellulose acetate^a			
CO ₂	1.43	34.2	0.197
Polycarbonate			
N ₂	0.0909	2.11	0.0564
CO ₂	0.685	18.81	0.262
Poly(2,6-dimethyl-1,4-phenylene oxide)			
CH ₄	0.33	18.1	0.11
CO ₂	0.95	27.5	0.25
Poly(methyl methacrylate)			
N ₂	0.020	1.902	0.043
CH ₄	0.102	8.507	0.046
CO ₂	0.944	19.680	0.158
Polysulfone			
N ₂	0.0753	9.98	0.0156
CO ₂	0.664	17.8	0.326
Poly(vinyl chloride)			
N ₂	0.0169	0.451	0.0448
CO ₂	0.587	8.939	0.2094

^a Data obtained at 30°C.

The fundamental law for transport through a flat membrane is given by *Fick's first law* as

$$J = -D \frac{dC}{dx} \quad (12.11)$$

where J is the flux (units of mass per unit time), D is the diffusion coefficient, and dC/dx is the concentration gradient of penetrant across the membrane. Integration of eq. (12.11) from $x = 0$ to $x = \ell$, using Henry's law for C (eq. (12.8)), and assuming that D is independent of concentration, gives

$$J = \frac{SD}{\ell} (p_2 - p_1) \quad (12.12)$$

where p_1 and p_2 are the pressure at the low- and high-pressure sides of the membrane, respectively. Substitution of $P = SD$ (eq. (12.7)) into eq. (12.12) gives

$$J = \frac{P}{\ell} \Delta p \quad (12.13)$$

which is equivalent to eq. (12.1).

Equations (12.11) and (12.12) strictly apply to the diffusion of gases at low to moderate pressures through rubbery polymers where Henry's law is valid and the diffusion coefficient is independent of concentration. For glassy polymers, the concentration of gases at low to moderate pressures is no longer given by Henry's law but by the dual-mode model (eq. (12.9)). The most successful approach to predict gas permeability in glassy polymers, the *partial immobilization* theory [8], is based upon the dual-mode model, which postulates that there are two populations of sorbed gas—the Henry's law dissolution component and Langmuir sites. In the partial immobilization theory, each population is assigned separate diffusion coefficients, for which Fick's first law can be written as

$$J = -D_D \left(\frac{dC_D}{dx} \right) - D_H \left(\frac{dC_H}{dx} \right) \quad (12.14)$$

where D_D and D_H are the diffusion coefficients for the Henry's law dissolution and hole populations, respectively. Generally, the diffusion coefficient for gas molecules contained in the Langmuir sites is smaller than that for the Henry's law regions. For example, $D_D = 5.15 \times 10^{-8} \text{ cm}^2 \text{ s}^{-1}$ and $D_H = 5.83 \times 10^{-9} \text{ cm}^2 \text{ s}^{-1}$ for polycarbonate at 35°C. Integration of eq. (12.14) and using the dual-mode model for C_D and C_H (eq. (12.9)) gives the expression for permeability as

$$P = k_D D_D \left(1 + \frac{FK}{1 + bp_2} \right) \quad (12.15)$$

where

$$F = \frac{D_H}{D_D} \quad (12.16)$$

and

$$K = \frac{C_H' b}{k_D}. \quad (12.17)$$

Equation (12.15) was obtained by assuming a pressure of p_2 at the high-pressure side of the membrane and zero pressure at the downside. For the example of polycarbonate cited above, the ratio of the diffusion coefficients, F , given by eq. (12.16), is 0.113. It is noted that as temperature increases to above T_g the polymer passes from the glassy to the rubbery state (see Section 4.3) and the Langmuir-capacity term, C_H' , and, therefore, K , goes to zero, and $P = k_D D \equiv SD$ (eq. (12.8)).

Both the permeability and diffusion coefficients can be determined by measuring the amount, Q_t , of permeant passing through a membrane at some time, t , as illustrated in Figure 12-11. From the steady-state transport rate, $(dQ_t/dt)_{ss}$, the permeability is determined as

$$P = \left(\frac{\ell}{p_2 A} \right) \left(\frac{dQ_t}{dt} \right)_{ss} \quad (12.18)$$

where A is the surface area of the membrane of thickness ℓ . The diffusion coefficient, which influences the initial or transient permeation behavior of the membrane, is obtained from measurement of the *time lag* (θ), which is the extrapolated value of Q_t , as shown in Figure 12-11. In the partial-immobilization model, the diffusion coefficient is related to the time lag as

$$\theta = \frac{\ell^2}{6D} [1 + f(K, F, bp_2)] \quad (12.19)$$

where $f(K, F, bp_2)$ is a function of the dual-mode parameters and pressure. For rubbery polymers where $C_H' = 0$, this term is zero and, therefore, the diffusion coefficient is simply obtained as

$$D = \frac{\ell^2}{6\theta}.$$

(12.20)

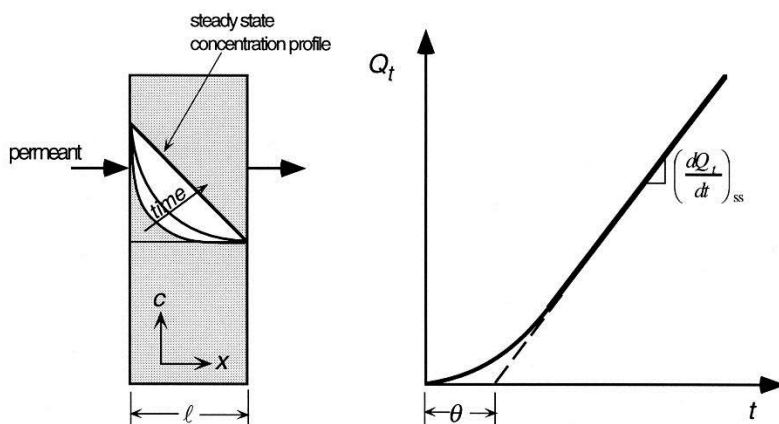


Figure 12-11 Plot of the amount of permeant versus time for a flat film illustrated at the left. The slope of the linear portion of the curve gives the steady-state permeability, while the intercept with the time axis yields the time lag, θ , from which the apparent diffusion coefficient can be obtained (eq. (12.20)). The increase in permeant concentration in the film up to the attainment of steady state is illustrated at the left.

Facilitated and Coupled Transport. As described in the previous sections, the basis of separation by filtration is particle size, while gas separation and pervaporation use differences in solute solubility and diffusivity to separate components from a mixture. In contrast, transport in two related processes—facilitated and coupled transport—is by means of a carrier mechanism. In both processes, a macroporous membrane (e.g., Celgard macroporous polypropylene) containing a free mobile carrier separates two liquid phases. The carrier, which is insoluble in the liquid phase, is contained in the membrane pores by capillary attraction. In facilitated transport, the carrier interacts with the permeant at the membrane–liquid interface. The permeant–carrier complex diffuses through the membrane and the permeant is released at the opposite membrane–liquid interface. An example of facilitated transport is the transport of oxygen by hemoglobin, as illustrated in Figure 12-12A. In the case of coupled transport, a chemical reaction occurs at the interface of the membrane and liquid phases, and mass flux occurs in both directions, as illustrated for $\text{Cu}^{2+}/\text{H}^+$ transport in Figure 12-12B. One practical problem with facilitated and coupled transport is the instability of the membrane, as the carrier may diffuse out of the pores of the macroporous membrane with time.

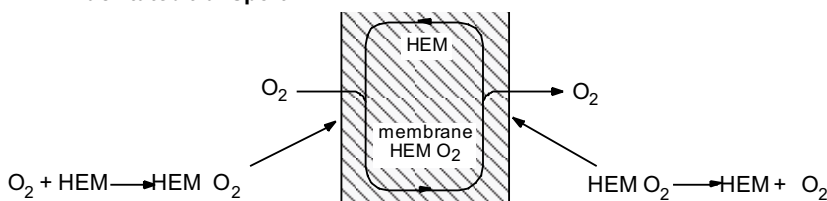
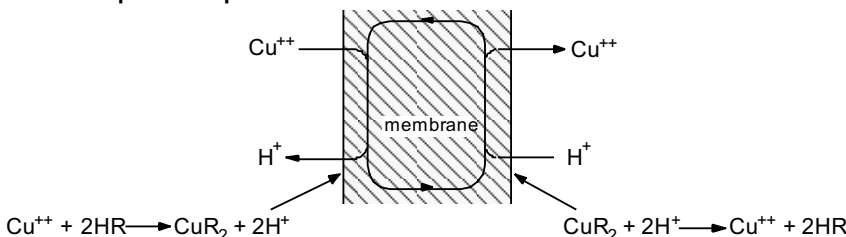
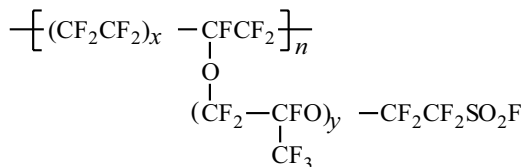
A Facilitated transport**B Coupled transport**

Figure 12-12 **A.** Facilitated transport of oxygen. **B.** Coupled transport of cupric and hydrogen ions. (Courtesy of Membrane Technology and Research, Inc., Menlo Park, CA).

Transport through Perfluorosulfonate Ionomers. As mentioned earlier, a class of polymers frequently used for a number of membrane-separation processes, including the chlor-alkali process, fuel cells, facilitated gas transport, and liquid separations, is the perfluorosulfonate ionomers (PFSI). As discussed in Section 10.2.2, PFSIs are copolymers of tetrafluoroethylene and a perfluorinated vinyl ether containing a terminal sulfonyl fluoride (SO_2F) group (structure 3).



3

The most important commercial PFSI product is Nafion ($y=1$), which is produced as film by melt extrusion. After film formation, the sulfonyl fluoride groups are converted to sulfonate groups by reaction with sodium or potassium hydroxide, with further conversion to the commercial sulfonic acid (SO_3H) form (Nafion-H). Other ionic forms (e.g., Na^+ , Li^+ , K^+ , Ag^+ , Ca^{2+} , Al^{3+} salts) can be obtained by ion

exchange with the appropriate salts. The importance of Nafion to chlor-alkali production is its selective permeability to ions. The morphology of Nafion membranes has been extensively studied to understand its transport properties. A widely accepted theory is the cluster-network model [9] illustrated in Figure 12-13. According to this model, the ionic sites (SO_3^-) of the pendant groups phase-separate from the polytetrafluoroethylene backbone to form clusters approximately 4 nm (40 Å) in diameter and connected by short, narrow channels. The ionic channels provide a relatively free diffusional path for cations such as Na^+ , for which it is highly selective. By the same reasoning, small polar molecules such as water and aliphatic alcohols easily pass through the ionic channels, while the diffusion of larger nonpolar molecules is restricted.

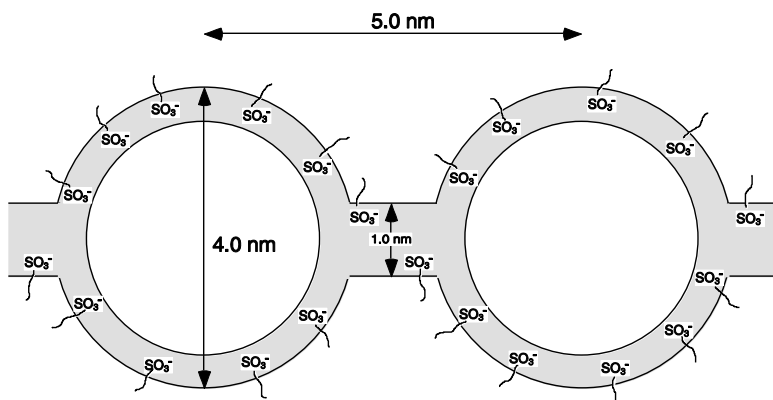


Figure 12-13 Illustration of the cluster-network model of perfluorosulfonate membranes [9].

12.1.4 Membrane Preparation

Dense membranes may be formed by any of the methods normally used to prepare films. These include melt extrusion, compression molding, and solution casting (see Chapter 11). As described next, procedures to prepare microporous and asymmetric membranes that consist of an integral dense skin covering a microporous substrate require significant art, as well as a basic understanding of polymer morphology and solution thermodynamics.

Microporous Membranes. Techniques that can be used to prepare microporous and ultraporous membranes are summarized in Table 12-8. Some microporous membranes suitable for ultrafiltration and microfiltration applications are prepared by stretching a semicrystalline polymer film such as a polyolefin (e.g., Celgard polypropylene) or polytetrafluoroethylene (e.g., Gore-Tex) in the solid

state. Stretching forces a separation of crystalline lamellae (see Section 4.2.1) and results in the creation of slit-like pores, typically $0.2 \text{ }\mu\text{m}$ in length and $0.02 \text{ }\mu\text{m}$ in width. Total porosity of such microporous membranes may be 40%.

Table 12-8 Methods Used to Prepare Microporous and Ultraporous Membranes

Method	Description
Leaching	Extraction of solid pore formers
Phase inversion	Phase separation of a ternary mixture of polymer, solvent, and nonsolvent
Sintering	Melting of a semicrystalline polymer powder
Stretching	Combined stretching and annealing of extruded semicrystalline film
Thermally induced phase separation	Cooling a mixture of a polymer with a latent solvent to a point of thermal separation of the mixture followed by extraction of the latent-solvent phase
Track etching	Irradiation of polymer films resulting in the production of fission fragments followed by caustic etching

Pore structure can also be obtained by leaching solids dispersed in a solid material by use of a suitable extraction solvent. For example, porous (“thirsty”) glass (e.g., Vicor glass) can be prepared by extracting boron-containing compounds and alkali metal oxides from hollow glass fibers with dilute hydrochloric acid. A pore size of approximately 40 \AA and a 40% void volume can be obtained by this procedure.

Microporous membranes can be prepared from a wide variety of thermoplastics by irradiation. This process is called nucleation track etching. When radioactive elements decay, fission fragments including heavy positive ions are produced that can penetrate polymers to significant depths. For example, fission fragments from ^{252}Cf can penetrate polycarbonate to a depth of $20 \text{ }\mu\text{m}$ while those from ^{235}U will penetrate to a depth of 10 to $12 \text{ }\mu\text{m}$. Collision of the fragments with polymer chains results in chain scission along the penetration path (see Chapter 6). These radiation-degraded polymer molecules are then etched from the film by treatment with acid or base. If the films are sufficiently thin compared to the depth of penetration, the combination of track formation and etching results in the creation of cylindrical pores that pass completely through the film and have a narrow pore-size distribution. Typical pore diameters fall in the range from 0.02 to $20 \text{ }\mu\text{m}$. In addition to polycarbonate, other polymers that can be track-etched include poly(ethylene terephthalate), cellulose acetate, cellulose nitrate, and poly(methyl methacrylate).

Asymmetric-Membrane Formation. In order to ensure favorable economics for membrane separations compared to other, more traditional separation techniques, it is necessary to achieve both high selectivity *and* high flux. While permea-

bility and selectivity of dense membranes are intrinsic properties of the membrane material, flux can be increased by decreasing the membrane thickness (eq. (12.12)). Since membranes must be sufficiently strong to withstand significant pressure drops (e.g., potentially as high as 2000 psi in some applications), there is a limit to how thin a membrane can be and still provide the necessary strength under operating conditions. A major technological advance that has addressed this problem was the development of asymmetric membranes in 1960 by Loeb and Sourirajan [10] for reverse-osmosis applications. As described next, these membranes are prepared by a phase-inversion process that produces a thin, dense surface layer or *skin* and a thick, macroporous substrate. The skin, which may be only 0.1 to 1 μm in thickness, provides the separating function while the substrate provides the mechanical strength. An electron micrograph of a typical asymmetric fiber is shown in Figure 12-14.

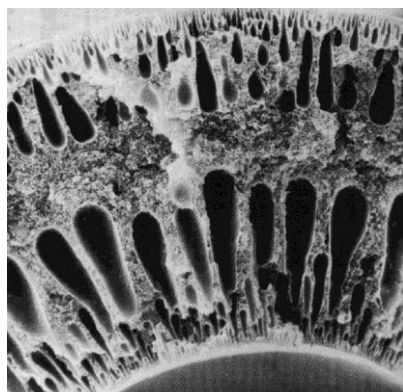


Figure 12-14 Photomicrograph of a cross section of an asymmetric hollow-fiber membrane showing large macrovoids in a porous substructure and a thin, dense skin on the outer and inner surfaces of the fiber. Reprinted with permission from J. M. S. Henis and M. K. Tripodi, *The Developing Technology of Gas Separating Membranes*. *Science*, 1983. **220**: p. 11. Copyright 1983 American Association for the Advancement of Science.

There are four techniques by which asymmetric membranes can be prepared—dry, wet, thermal, and polymer-assisted. All involve the phase separation of a moderately concentrated polymer solution to form a gel in which the polymer becomes the continuous phase and solvent molecules coalesce to form pockets. Removal of the solvent from these pockets leaves voids, which constitute the macroporous structure of the asymmetric membrane. Phase inversion can be induced either by the action of a nonsolvent such as water (i.e., chemically induced) or by a change in temperature (i.e., thermally induced), which causes the membrane solution to become thermodynamically unstable and consequently to phase-separate (see Chapter 3).

In the dry process of membrane formation, a polymer, solvent, and nonsolvent are mixed to give a composition within the miscible or single-phase region of the triangular diagram, as shown in Figure 12-15. The solution is then evaporated to dryness. As the volatile components (i.e., solvent and nonsolvent) are lost, the overall composition moves into the miscibility gap and phase separation occurs. In the wet process, a polymer solution is partially evaporated and then coagulated in a nonsolvent, typically water.

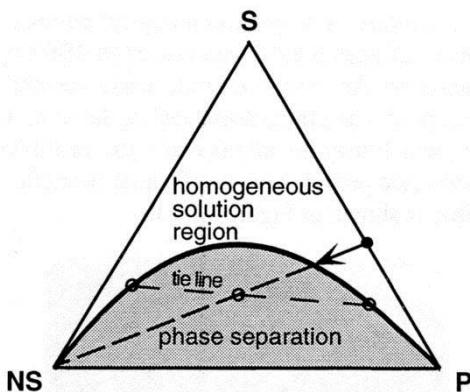


Figure 12-15 Phase diagram of a ternary mixture containing polymer (P), solvent (S), and nonsolvent (NS) at constant temperature. When a nonsolvent is added to a concentrated polymer solution whose composition is indicated by the filled circle along the S-P side, the overall composition of the mixture follows the line connecting this point and the NS vertex. When the composition reaches the phase envelope, phase separation (coagulation) begins. The composition of the two equilibrium phases is given by a tie line through the point on the phase diagram representing the overall composition of the ternary mixture, as shown.

The thermal process or thermally induced phase separation (TIPS) utilizes a “latent” solvent and a decrease in temperature to cause phase separation. A latent solvent is one that has a high-boiling-point, low-molecular-weight solvent for the polymer at some high temperature (e.g., 220°C) but a nonsolvent at lower temperature. Examples of latent solvents include *N*-tallowdiethanolamine (TDEA), menthol, and sulfolane. The polymer and latent solvent are melt-blended, cast into a film or extruded as a fiber, and then cooled to induce phase separation. As shown in Figure 12-16, phase separation occurs when the temperature is lowered to below the upper critical solution temperature (UCST). After phase inversion, the latent solvent (the pore former) is then extracted by another solvent (a nonsolvent for the polymer). Membrane morphology is determined by many parameters, such as the polymer concentration, solution temperature, and rate of cooling. Phase separation within the spinodal results in phase separation by a mechanism called *spinodal decomposition*.

Spinodal decomposition results in a “lacy” membrane structure. Phase separation within the metastable region located between the spinodal and binodal occurs by nucleation and growth and leads to an open pore structure. Microporous membranes of high-density polyethylene, polypropylene, polystyrene, and poly(2,6-dimethyl-1,4-phenylene oxide) can be prepared by this procedure.

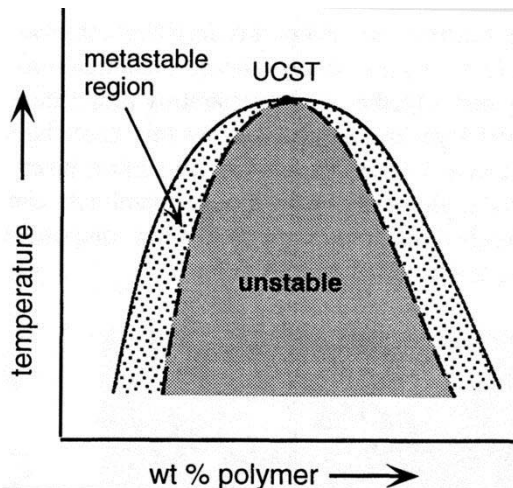


Figure 12-16 Phase diagram of a polymer solution illustrating phase separation as temperature decreases below the upper critical solution temperature (UCST). The binodal is indicated by the solid curve; the spinodal is represented by the broken curve.

The polymer-assisted method of membrane formation utilizes a mixture of *two* physically compatible but immiscible polymers dissolved in a common solvent. This means that the two polymers form a homogeneous solution with the solvent at low to moderately high polymer content but do not form a homogeneous mixture in the solid state. When the solution is cast and the solvent evaporated, phase separation of the two polymers results. The polymer with lower concentration in the blend will form the dispersed phase in a continuous phase of the polymer present in higher concentration. The art is to select the dispersed-phase polymer to be soluble in some convenient solvent (usually water) that is not a solvent for the polymer forming the continuous phase. An example of a water-soluble polymer that is used for this purpose is poly(*N*-vinylpyrrolidone) (PVP). After casting and drying, the dispersed phase is extracted out of the membrane by the solvent. The resulting membrane will have a skinless, microporous structure suitable as a substrate for the preparation of composite membranes.

Coated Asymmetric and Composite Membranes. Although asymmetric membranes have great potential as highly efficient membranes for gas separations,

small defects or pores can develop in the skin layer during their preparation. These pinholes permit the free passage of gas molecules through the membrane, resulting in reduced separation. Such pores need to be only approximately 10 Å or more in diameter to cause a significant decrease in selectivity. The problem of achieving defect-free skinned membranes was solved by Henis and Tripodi [11] who showed that coating an asymmetric fiber with a thin layer of a highly permeable polymer such as silicone rubber plugged the open pores and forced separation to occur through the dense, separating region of the skin.

Membranes with attractive flux and permselectivity can also be prepared by using a microporous membrane (e.g., a skinned asymmetric membrane) as a support for casting a thin film of another polymer with the desired separation properties. A composite membrane with a very thin separating layer can be obtained by this procedure. Alternatively, lamination and plasma polymerization can be used to prepare the surface layer. The membrane flux and permselectivity of a coated asymmetric or composite membrane can be related to membrane morphology and the individual transport properties of the components by analogy to an electrical-resistance network, as illustrated by Figure 12-17.

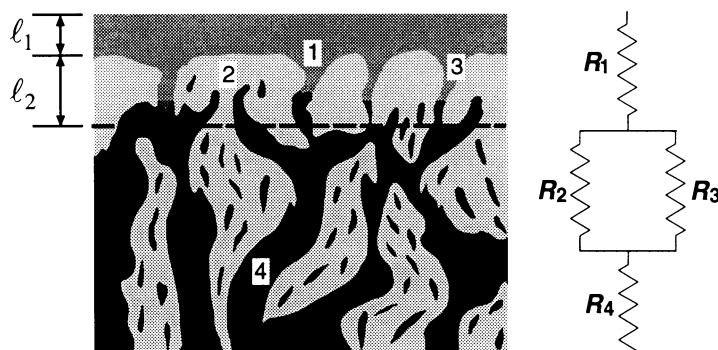


Figure 12-17 The resistance model of coated asymmetric membranes: coating (1), dense layer (2), pore (3), and substrate (4). Adapted from M. S. Henis and M. K. Tripodi, *Composite Hollow Fiber Membranes for Gas Separation: The Resistance Model Approach*. Journal of Membrane Science, 1981. **8**: p. 233. Copyright 1981, with permission from Elsevier.

In the resistance model, the permeation flux

$$Q_i = \left(\frac{P_i}{\ell} \right) A \Delta p \quad (12.21)$$

is equated with electrical current, I , and the driving force or pressure drop, Δp , across the membrane with the electrical potential, E . In an electrical network, the resistance, R_e , is related to I and E by Ohm's law

$$R_e = \frac{E}{I}. \quad (12.22)$$

It follows that the analogous resistance to permeation, R_p , is given as

$$R_p = \left(\frac{\ell}{P_i} \right) A. \quad (12.23)$$

The coated membrane illustrated in Figure 12-17 is equivalent to a resistor (dense coating layer, 1) in series with two parallel resistors (i.e., the dense layer, 2, and the pore region, 3, of the skin) and with the porous substrate, 4. The total resistance of the network is then given as

$$R_T = R_1 + \frac{R_2 R_3}{R_2 + R_3} + R_4. \quad (12.24)$$

The substrate is typically sufficiently porous to pose no significant resistance to permeation (i.e., $P_4 A_4$ is very large) and, therefore, R_4 may be safely neglected. To simplify the analysis, it may be assumed that the smaller pores in the skin are filled completely with the coating material to the depth of the skin (ℓ_2) although it can be shown that, in usual circumstances, complete filling is not required for the coating to be effective. Furthermore, the pore area, A_3 , is typically only a small fraction of the total surface area of the fiber (i.e., $A_2 \gg A_3$) and, therefore, $A_2 \approx A_1$. Using these assumptions, the resulting equation for total membrane flux becomes [11]

$$\frac{Q_i}{A_2 \Delta p} = \left(\frac{P}{\ell} \right)_i = \left[\frac{\ell_1}{P_{1,i}} + \frac{\ell_2}{P_{2,i} + P_{1,i}(A_3/A_2)} \right]^{-1}. \quad (12.25)$$

Values of P/ℓ for the coating and substrate polymers may be easily obtained from steady-state permeability measurements of dense films of the two materials and the fiber morphology (e.g., A_3/A_2 , ℓ_1 , and ℓ_2) can be determined by electron microscopy.

Module Fabrication. For commercial separations of liquids and gases and for purification and desalination of seawater, membranes with very large surface areas (10^3 to 10^7 m^2) and high area-to-volume ratios (packing density) are needed to meet flux requirements. A hollow-fiber membrane module illustrated in Figure 12-18 gives the highest packing densities (10^4 to $10^5 \text{ m}^2 \text{ m}^{-3}$). Other configurations include spiral-wound, plate-and-frame, tubular, and capillary. Typical module designs used

for reverse osmosis (RO), pervaporation (PV), gas permeation (GP), ultrafiltration (UF), electrodialysis (ED), and microfiltration (MF) are given in Table 12-9.

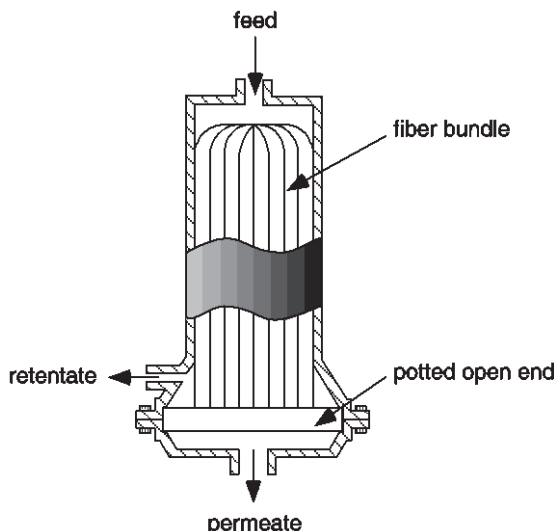


Figure 12-18 Cutaway view of a typical hollow-fiber membrane module. Adapted from K. Scott, *Membrane Separation Technology*. 1990, Oxford: STI.

Table 12-9 Preferred Module Designs for Major Membrane Separations

Module Type	Separation ^a
Capillary	UF, MF
Hollow-fiber	RO, GP, PV
Plate-and-frame	PV, UF, ED
Spiral-wound	RO, PV, GP
Tubular	UF, MF

^a Code: RO, reverse osmosis; GP, gas permeation; PV, pervaporation; UF, ultrafiltration; ED, electrodialysis; MF, microfiltration.

Hollow-fiber modules are frequently used for commercial RO and gas separations. The typical o.d. of hollow fiber ranges from 80 to 200 μm with a wall thickness of 20 μm or greater. These fibers are made (melt or wet spinning) from polyamide, cellulose triacetate, and sulfonated polysulfone for RO applications and usually polysulfone for gas separations. Seals for membrane bundles are usually made from epoxy. Modules containing fibers of larger diameters are sometimes called *capillary modules* and are used for UF (and MF) applications. Typical polymers used for UF capillary modules include polysulfone, polyacrylonitrile, and chlorinated polyolefins. In all cases, process streams must be pretreated to remove large par-

ticles that can plug pores or chemicals that can dissolve or craze the polymeric fibers or lead to swelling or leakage of the seal materials.

The principal application for *spiral-wound membranes* has been reverse osmosis. As illustrated in Figure 12-19, spiral-wound modules are prepared by sandwiching alternate layers of flat sheet membranes, spacers, and porous material around an inner porous permeate-collection tube. The feed flows axially along the sandwich in the channels, approximately 1.0 mm in depth, formed by the spacers, while the permeate flows radially to the collection tube. Spiral-wound membrane modules designed for RO separations are typically about 1 m in length and 0.2 m in diameter and can accommodate flow rates up to 28 m^3 per day and pressures up to 40 bars.

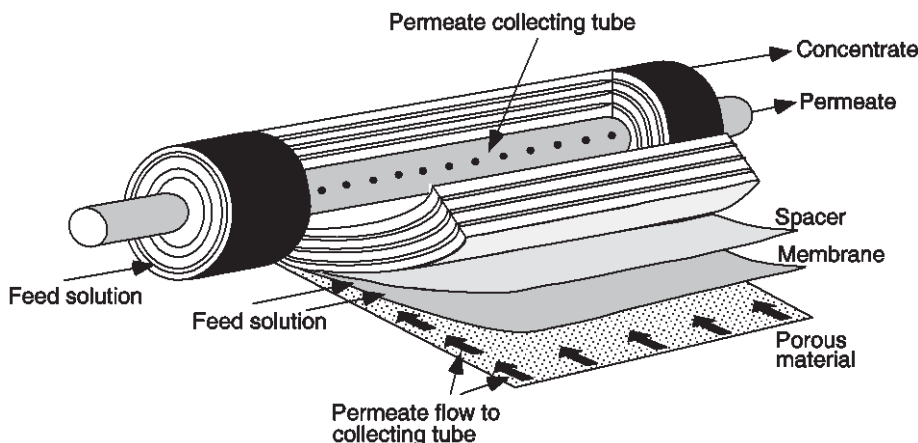


Figure 12-19 Spiral-wound membrane modules. Adapted from K. Scott, *Membrane Separation Technology*. 1990, Oxford: STI.

In cases where feeds cannot be pretreated to remove potential fouling contaminants or where the module must be steam-sterilized, a tubular-membrane module, as illustrated in Figure 12-20, is sometimes used. The module, which looks much like a shell-and-tube heat exchanger, consists of an inner membrane tube surrounded by porous supporting tubes. In some cases, the membrane may be inorganic (e.g., ceramic) rather than organic to meet the more aggressive environments in which such modules are used. Such units can be easily cleaned and can be steam-sterilized; however, pressure losses are high and productivity is low compared to hollow-fiber and spiral-wound units. Principal applications for tubular-membrane modules are UF and MF.

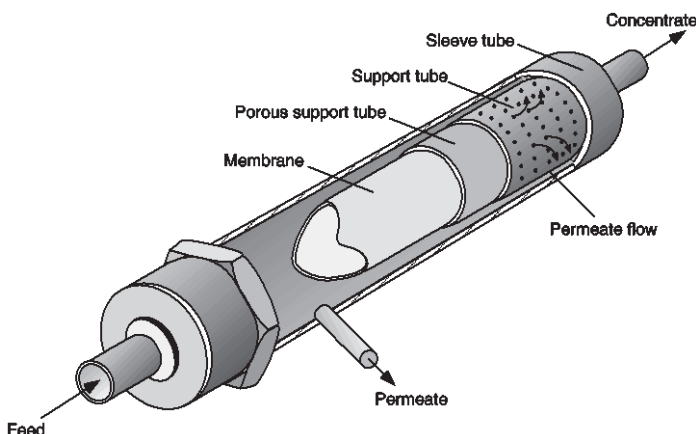


Figure 12-20 Tubular-membrane module. Adapted from K. Scott, *Membrane Separation Technology*. 1990, Oxford: STI.

12.2 Biomedical Engineering and Drug Delivery

Polymers are widely used in medicine as materials in the manufacture of sutures, vascular grafts, intravascular stents, artificial organs, orthopedic implants, and prosthetic devices. Polymers also find applications in controlled release of drugs as an alternative to more traditional metal amalgams. Depending upon the application, polymers for biomedical use must be biocompatible and excel in properties specific for the specific application such as selective permeability, biodegradability, and high strength or modulus. The biocompatibility of a polymeric material depends upon the degree of adsorption of plasma proteins to the polymer surface and upon the interaction of these proteins with cell receptors. Protein adsorption can be reduced by increasing hydrophilicity or steric repulsion using plasma film deposition and by the grafting of water-soluble polymers, such as the radiation grafting of *N*-allylacrylamide. Segmented polyurethanes and poly(urethane-urea) are examples of polymers having good biocompatibility that can be further improved through grafting of heparin, a D-glucosamine polysaccharide.

Polymers that have been used in medical applications include PVC, polypropylene, some acrylics, and polystyrene. Radiation-sterilizable and environmentally safe grades of PVC have given this polymer a significant share of the medical plastics market. Polypropylene has been used in sterilizable medical packaging and drug-delivery devices. Recent metallocene polyolefins (see Section 2.2.3) provide some advantages for medical applications including superior optical clarity, ductility at low temperature, and low residual concentration of polymerization catalysts. The attractive properties of metallocene-polymerized syndiotactic polystyrene (see

Section 9.1.2) such as its high thermal stability open opportunities for use as sterilizable trays, surgical instruments, and dental equipment.

Polymers can be used in the treatment of diseases including cancer [12] through facilitated and safe delivery of drugs (e.g., paclitaxel), proteins, and genetic material such as DNA (gene therapy). As illustrated in Figure 12-21, hydrophilic polymers may be used to link a specific drug (Figure 12-21a), to engulf a protein (Figure 12-21b) or a recombinant DNA sequence (Figure 12-21c), and to enclose a poorly soluble (hydrophobic) drug within a micelle (Figure 12-21d) or a dendrimer (Figure 12-21e). Natural and synthetic polymers and copolymers that have been evaluated for these applications include poly(ethylene glycol) (PEG), *N*-(2-hydroxypropyl) methacrylate copolymers, poly(vinyl pyrrolidone), poly(ethylene-imine) (PEI, structure 4), polyphosphazenes, hyaluronic acid, chitosan, dextran, poly(aspartic acid), poly(L-lysine) (PLL, structure 5), and poly(lactic-*co*-glycolic acid). PEG, being nontoxic and non-immunogenic, is a particularly common polymer used in graft and block copolymers. PEG is often used to water-solubilize a variety of drugs, proteins, and several nanoparticles. Triblock copolymers of PEG with poly(ϵ -caprolactone) (PCL), PEG-*b*-PCL-*b*-PEG, and with poly(D,L-lactic acid-*co*-glycolic acid), PEG-*b*-PLGA-*b*-PEG, can form polymeric micelles that can encapsulate a drug. A commonly used dendrimer is polyamidoamine (PAMAM). Applications of polymers in controlled drug delivery, gene therapy, antibiotic fibers and fabrics, tissue engineering, kidney dialysis, and artificial organs are discussed in the following sections.

12.2.1 Controlled Drug Delivery

Controlled drug delivery, or controlled release, provides two important potential applications for the use of polymers in the effective management of medical drugs in the body. The first of these is *controlled release* whereby a steady therapeutic concentration of the drug is maintained. Current examples of the use of controlled drug release include the delivery of contraceptives and the treatment of glaucoma. The other application is *site-directed* drug delivery whereby a polymer serves as a carrier to bring a drug to a specific site in the body, such as a site of infection, a diseased organ, or a collection of malignant cells.

Drugs can be delivered in a variety of traditional forms such as tablets, pills, capsules, liquids, and injections. While polymers are sometimes used as binders to modify consistency or to contain a specific dosage, they can also be used to deliver and target drugs in some applications. Polymers for such applications must be biocompatible and be able to biodegrade into products that are nontoxic and biocompatible themselves. Those that meet these requirements include a number of hydrolysable polyesters such as PLA and PGA and block copolymers of the two. Other choices include polyanhydrides, polyphosphoesters, poly(amino acids), and chitosan. PEG has been used to attach drugs. Styrene-isobutylene block copolymers

have been used as a cardiac stent coating for the controlled delivery of the drug Taxol (paclitaxel), which serves to prevent the narrowing of the arteries due to restenosis whereby the migration of vascular smooth-muscle cells can restrict blood flow.

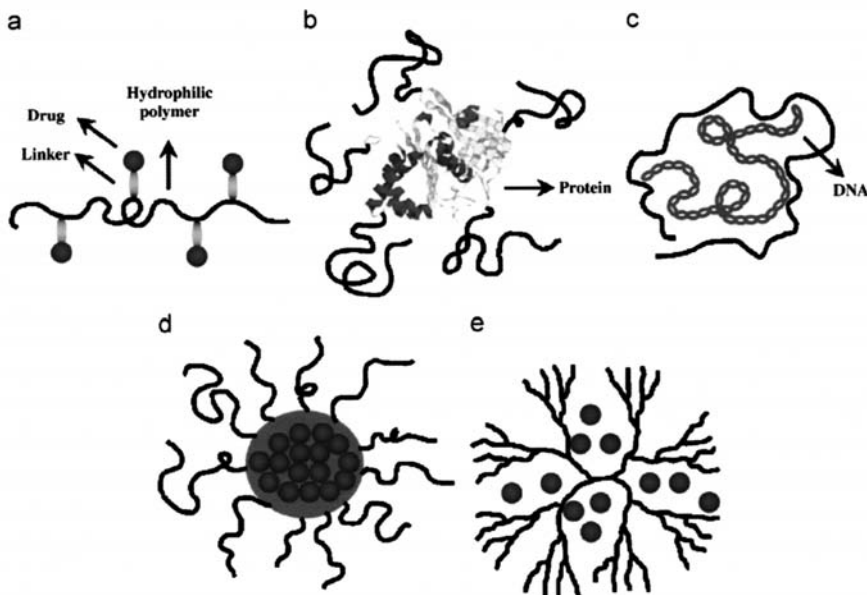
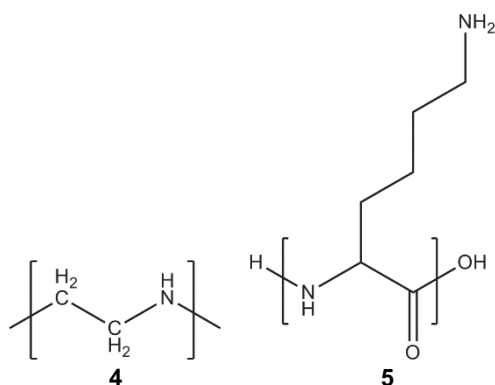


Figure 12-21 Illustration of polymeric nanomedicines: (a) polymer–drug conjugates; (b) polymer–protein conjugates; (c) polymer–DNA conjugates; (d) polymeric micelles; and (e) dendrimers. Reproduced from J. H. Park et al., *Polymeric Nanomedicine for Cancer Therapy*. Progress in Polymer Science, 2008. 33: p. 113–137. Copyright 2008, with permission from Elsevier.

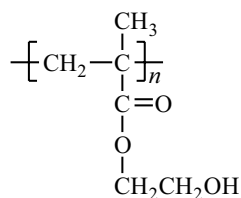


The rate of drug release can be controlled by diffusion, reaction, or solvent. In *diffusion control*, the driving force for diffusion is the concentration gradient across the delivery device, which can be a reservoir or matrix system. In the reservoir system, the drug is encapsulated by a polymeric membrane, which can be either microporous or nonporous. Delivery is constant in time if the drug core is maintained at a saturated level. In the case of a matrix system, the drug is dissolved or dispersed in a polymer. In contrast to the reservoir system, the release rate in a matrix device will decrease with time as the distance the drug has to travel from within the matrix increases due to depletion of drug concentration at the surface of the device. Polymers that have been used for diffusion-controlled devices include polydimethylsiloxane and poly(ethylene-*co*-vinyl acetate).

Reaction-controlled systems utilize biodegradable polymers as a means of delivery. The drug can be physically dispersed in the polymer, which gradually degrades in the body as a result of hydrolysis or enzymatic attack. Alternatively, the drug can be chemically linked to a polymer chain by a suitable spacer group that provides a biodegradable link. For reaction-controlled delivery, poly(lactide-*co*-glycolide) is particularly attractive because its breakdown products, lactic and glycolic acids, are biologically safe.

In *solvent-controlled* delivery, drug release is regulated by the permeation of water through the polymer. This may be achieved by the use of a simple osmotic pump, as illustrated in Figure 12-22. In this example, the drug core is enclosed by a semipermeable membrane that allows water to penetrate into the device due to osmotic pressure. The drug solution is dispersed through the orifice of the device at a rate equal to the rate of water uptake.

Another type of a solvent-activated system for controlled release uses polymeric *hydrogels*, which are water-swollen crosslinked polymer networks. The drug is incorporated in hydrogel polymer in the dry (glassy) state. When introduced in an aqueous environment, the polymer swells. The resulting gel provides a medium favorable for drug diffusion. A commonly used hydrogel is prepared from poly(2-hydroxyethyl methacrylate) (PHEMA, structure 6) crosslinked by copolymerization with a difunctional polymer. Since PHEMA is water soluble, the crosslinked network will swell to form a gel containing about 35% water in an aqueous environment. In addition to controlled-release applications, PHEMA is used in the manufacture of soft contact lenses.



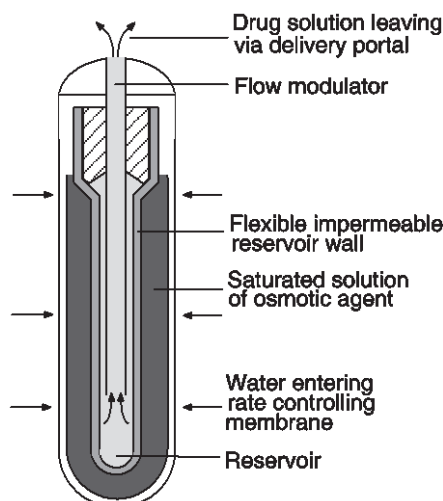


Figure 12-22 Illustration of an osmotic pump used in controlled drug delivery. Reprinted with permission from ASTM Standardization News, October 1986. Copyright ASTM International, 100 Barr Harbor Drive, West Conshohocken, PA 19428.

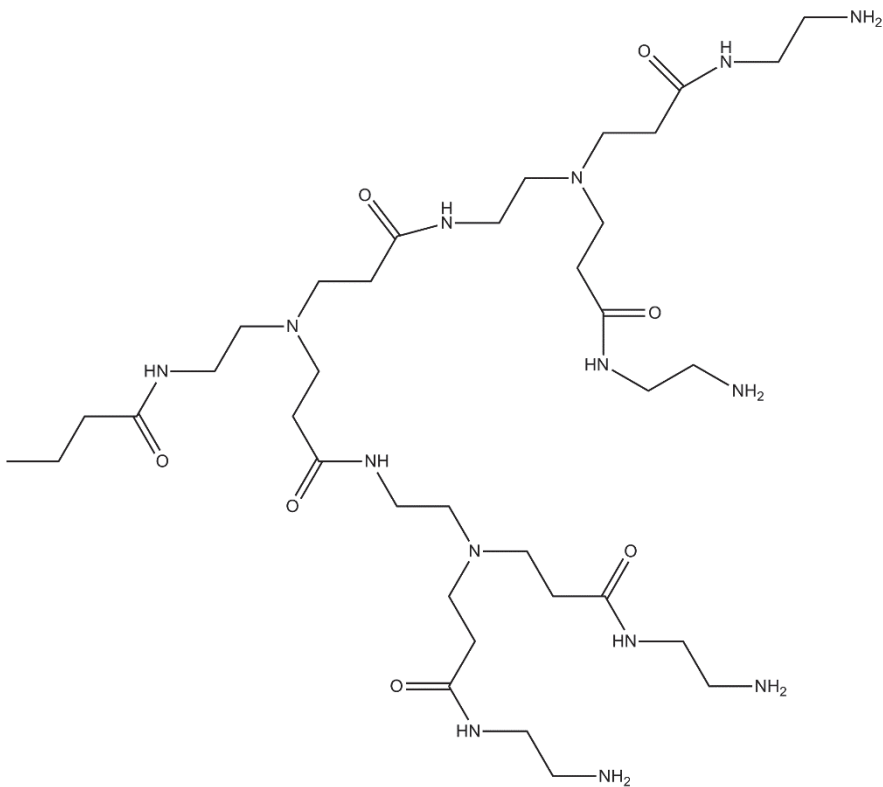
Although the technology for *site-directed drug delivery* is still in its infancy, some examples illustrate its potential. One application uses a block copolymer of poly(ethylene glycol) (PEG) and poly(aspartic acid) as the drug carrier. PEG provides the carrier solubility, while the poly(amino acid) is used to attach an anti-cancer drug (e.g., adriamycin).

12.2.2 Gene Therapy

Gene therapy employs the transfer of genetic material, primarily plasmid DNA, to modify defective genes or to replace missing ones as an approach to treating disease. Carriers for this genetic material may be a recombinant virus or a synthetic vector such as a lipid, a polypeptide such as polylysine (shown in structure 5), or polymers that can complex with DNA (a polyplex). Viruses used as vectors can be made non-replicant (and, therefore, non-pathogenic) by replacing a part of the genome with a therapeutic gene. While viral vectors are extremely efficient due to the inherent engineering of a virus, there is a significant risk that the recombinant virus may revert to a wild-type virulent form. Fatalities have been reported in some clinical trials. For this reason, there is significant interest in developing safe synthetic vectors such as polymers. While polymeric vectors pose fewer risks, they are significantly less efficient than viral vectors. Early issues with this approach include low

efficiency, toxicity, and poorly understood delivery mechanisms. An excellent review of the subject has been given by Pack et al. [13].

Effective polymeric vectors must be able to electrostatically bind the DNA through cationic interaction with the negative phosphates along the DNA backbone (see Chapter 8, Section 8.1.2) forming nanoparticles that provide protection of the genetic material and enable transfection of the genetic material into the nucleus of the target cell. Delivery of DNA into the nucleus requires a complex process whereby the polyplex is incorporated into the cell through endocytosis and is then transported through the cytoplasm or along the microtubules into the nucleus. The efficiency of a successful transfer is very low (~1%). Polymers that have been considered for gene delivery include polylysine, polyethylenimine (PEI), and a starburst dendrimer of polyamidoamine, NR₃, for which the branched group, R, is shown in structure 7. While one of the earliest polymers evaluated, polylysine has very low efficiency. PEI is relatively effective but has high cytotoxicity. Polyamidoamine offers both good biocompatibility and efficiency. Biodegradable polymers, such as poly(β -amino esters) (PAE), that can hydrolyze into small metabolites having low toxicity have also been considered.



12.2.3 Antimicrobial Polymers

Antimicrobial polymers, sometimes called biocidal polymers, constitute a class of functionalized polymers that are able to inhibit the growth of bacteria and other microorganisms. Applications include biocidal fabrics and films, water sanitation, the prevention of infection in medical and dental practice, and the prevention of bacterial contamination in the food industry. An extensive review of the area has been given by Kenaway et al. [14]. To be effective, a polymeric biocide must be able to adsorb on the negatively charged cell membrane of a bacterium, disrupt the cell membrane, and cause lysis and cell death. In this way, they mimic the action of certain proteins such as gramicidin and magainin. Polymers that provide biocidal function include chitosan, polymeric quaternary ammonium materials, halogenated polystyrene–divinylbenzene sulfonamides, and polyurethanes having surface-active alkylammonium chloride end groups. Recently, a variety of nanocomposites containing silver nanoparticles, bioactive agents intercalated in montmorillonite (MMT, Section 7.5), and functionalized polyhedral oligomeric silsesquioxane (POSS) also have shown promise for their antimicrobial efficacy.

12.2.4 Tissue Engineering

The ability to repair or regenerate tissue has great importance for growing skin for the repair of burned areas, for the repair of damaged tendons, and for the growth of stem cells, as examples. For this purpose, it is necessary to support growing cells on a suitable *scaffold* structure. The scaffold serves as an immobilizing and protective site for transplanted cells and to direct cell growth through the transport of growth factors and other hormones and nutrients. The naturally occurring protein collagen is an excellent biomaterial for scaffold construction [15] but issues of contamination and infection limit its use as a scaffold material. An alternative approach is the use of biocompatible polymers for the construction of scaffolds to repair and regenerate tissue defects [16]. There are a number of requirements for polymers for such applications. They must be biodegradable, non-antigenic, non-carcinogenic, nontoxic, non-teratogenic, and biocompatible [17]. Polymers and copolymers that have been evaluated for scaffolds include trimethylene polycarbonates, polyphosphazenes, polyurethanes, polyfumarate, polyorthoester, poly(glycerol sebacate), polypyrrole, polyacrylates, poly(ether ester amide), poly(amido amine), and poly[(D,L-lactic acid)-*co*-(glycolic acid)] (PLGA).

12.2.5 Kidney Dialysis and Artificial Organs

Kidney Dialysis. One of the important medical applications of polymeric membranes is kidney dialysis, used to remove low-to-moderate-molecular-weight compounds from blood. These include sodium chloride, potassium chloride, urea, creatinine, and uric acid. At the same time, larger molecules necessary for life, such as cellular particles and plasma proteins, must be retained. The driving force for dialysis is a concentration gradient. Polymers suitable for kidney dialysis include cellophane (regenerated cellulose) that can be prepared in the form of small-diameter (ca. 200- μm) hollow fibers approximately 17 cm in length. As many as 10,000 of these fibers are used in a typical dialysis module. Practical problems that are encountered in operation include concentration polarization and clogged pores due to the adsorption of plasma proteins.

Artificial Organs. Some polymers can be used to manufacture artificial organs such as artificial kidneys, pancreases, and lungs. Artificial tendons and muscles have also been developed. A concern is always thrombus (clot) formation when foreign substances are in contact with blood. Heparin, a sulfonated glycosaminoglycan having anticoagulation properties, can be grafted onto the polymer surface to impart thrombo-resistance.

12.3 Applications in Electronics and Energy

Polymers can be electrically conductive or, doped with conductive fillers, can also be made photoconductive. These properties provide important applications such as polymeric electrodes in batteries, photovoltaics for solar cells, electronic shielding, encapsulation, and dielectrics as discussed in this section.

12.3.1 Electrically Conductive Polymers

In general, polymers have very poor electrical conductivity. In fact, some polymers such as polytetrafluoroethylene are good electrical insulators. In the 1800s, it was observed that the conductivity of natural rubber—normally an excellent insulator—could be significantly increased by adding carbon black, which is naturally conductive. In the 1930s, natural rubber filled with acetylene black was used in antistatic devices in hospitals and other facilities to reduce the danger of sparks resulting from the buildup of static electricity.

Before 1973, only one polymer—polysulfurnitride (SN_x)—was known to have any appreciable conductivity ($\sim 10^3 \text{ S cm}^{-1}$).^{*} As in the case of natural rubber, it was found that this conductivity could be increased significantly by doping with an electron acceptor such as bromine ($\sim 10^4 \text{ S cm}^{-1}$).[†] Unfortunately, interest in this polymer was less than it would otherwise be because of the explosive nature of its precursor monomer, S_2N_2 .

By the late 1970s, researchers in the United States and Japan had shown that the electrical conductivity of an organic polymer—polyacetylene—could also be increased by a factor of 10^{12} (to $\sim 10^3 \text{ S cm}^{-1}$) when it was doped with an electron donor such as an alkali–metal ion or an electron acceptor such as arsenic pentafluoride (AsF_5) or iodine.[‡] The conductivity of doped polyacetylene is comparable to that of copper on an *equal weight basis*. A comparison of the electrical conductivities and specific gravities of several polymers, common metals, and carbon is made in Table 12-10.

Table 12-10 Conductivities of Polymers and Metals

Material	Conductivity ^a (S cm^{-1})	Specific Gravity
Silver	10^6	10.5
Copper	6×10^5	8.9
Aluminum	4×10^5	2.7
Polyacetylene (doped)	1.5×10^5	1
Platinum	10^5	21.4
Polythiophene (doped)	10^4	1
Mercury	10^4	13.5
Carbon fiber	500	1.7–2
Carbon-black-filled polyethylene	10	1
Polymer electrolyte ^b	10^{-4}	1
Polytetrafluoroethylene (Teflon)	10^{-18}	2.1–2.3
Polyethylene	10^{-22}	0.9–0.97

^a Units of siemens (S) per cm.

^b Ionic conductivity.

* The basic unit of conductivity (the inverse of resistivity) is siemens (S) per cm. A siemens is a reciprocal ohm (i.e., $1 \text{ S} = \Omega^{-1}$). As an illustration, the conductivity of polytetrafluoroethylene, an excellent insulator, is approximately $10^{-18} \text{ S cm}^{-1}$.

† Polysulfurnitride has been observed to become superconductive ($\sim 108 \text{ S cm}^{-1}$) at temperatures approaching absolute zero. ($\sim 0.3 \text{ K}$).

‡ In 2000, Alan J. Heeger, Alan C. MacDiarmid, and Hideki Shirakawa shared the Nobel Prize in chemistry for their discovery and development of conductive polymers.

More recently, conductivity has been demonstrated for doped versions of poly(*p*-phenylene) (PPP), polypyrrole (PPy), polythiophene (PT), and polyaniline (PANI). The synthesis and properties of polyacetylene and these other conductive polymers were reviewed in Section 10.2.7. Although the electrical conductivities of many of these other polymers are lower than those polyacetylene, they have the advantage of being more stable against the effects of oxygen and moisture. As shown by the chemical structure of the repeating units of these polymers in Table 12-11, a common feature that makes these polymers capable of transporting electrical charge is a conjugated π -electron consisting of alternating single and double bonds along the polymer chain backbone or ring structure. It is believed that doping results in an electron imbalance, and the extended π -conjugated structure of the conductive polymer allows the new electron population to move along the backbone when an electric potential is applied.

In general, conductivity increases with decreasing *band gap*, which is the amount of energy needed to promote an electron from the highest occupied molecular orbital (HOMO), the valence band, to the lowest unoccupied molecular orbital (LUMO), empty band, immediately above it. The empty band is the conduction band. Metals have zero band gaps, while insulators like many polymers have large band gaps (1.5 to 4 eV), which impede electron flow. By careful design of the chemical structure of the polymer backbone, it may be possible to obtain band gaps as low as 0.5 to 1 eV. Currently, the lowest band gap observed for a polymer is \sim 1 eV reported for polyisothianaphthalene (see Table 12-11).

12.3.2 Polymeric Batteries

Potential applications of conductive polymers are significant since they are generally lighter, more flexible, and easier to fabricate than many of the materials they seek to replace. An important example is the use of polymers as both cathodes and solid electrolytes in batteries for automotive and other applications as alternatives to lead-acid batteries. A diagram of a typical lithium–polymer battery is shown in Figure 12-23. Potential advantages of polymeric batteries include high reliability, light weight, non-leakage of electrolyte solution, ultrathin-film form, flexibility, and high energy density (up to 100 W dm^{-3}). Polyacetylene, poly(*p*-phenylene), polypyrrole, and polyaniline can be used as the cathode material, with a lithium–aluminum alloy as the anode. Lithium–poly(*p*-phenylene) batteries can deliver current densities as high as 50 mA cm^{-2} , achieve efficiencies up to 91% during charging and discharging, and have theoretical energy densities of 320 W-h kg^{-1} . Examples of polymers used in the formulation of solid electrolytes include poly(alkyl sulfide)s, polyphosphazenes (see Section 10.2.5) having oligo(oxyethylene) side groups, and especially poly(ethylene oxide). Salts that are added to form the electrolyte include a number of lithium salts having low crystal lattice energies, such as lithium tetrafluoroborate

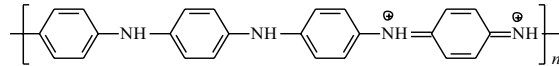
(LiBF₄), lithium hexafluoroarsenate (LiAsF₆), lithium perchlorate (LiClO₄), and lithium trifluoromethanesulfonate, sometimes called lithium triflate (LiCF₃SO₃).

Table 12-11 Chemical Structures and Conductivities of Some Electrically Conductive Polymers

Conductive Polymer	Repeating Unit	Dopants	Conductivity ^a (S cm ⁻¹)
<i>trans</i> -Polyacetylene		I ₂ , Br ₂ , Li, Na, AsF ₅	10 ⁴
Poly(3-alkyl-thiophene)		BF4-, ClO4-, FeCl4-	10 ³ – 10 ⁴
Polyaniline ^b		HCl	200
Polyisothianaphthalene		BF4-, ClO4-	50
Poly(<i>p</i> -phenylene)		AsF ₅ , Li, K	10 ³
Poly(<i>p</i> -phenylene vinylene)		AsF ₅	10 ⁴
Polypyrrole		BF4-, ClO4-, tosylate ^c	500–7500
Polythiophene		BF4-, ClO4-, tosylate ^c , FeCl4-	10 ³

^a Approximate maximum conductivity of doped polymer.

^b Polyaniline exists in four oxidation states, of which only the emeraldine salt



is a good conductor requiring only protonic doping of the imine nitrogen as shown.

^c *p*-Methylphenylsulfonate.

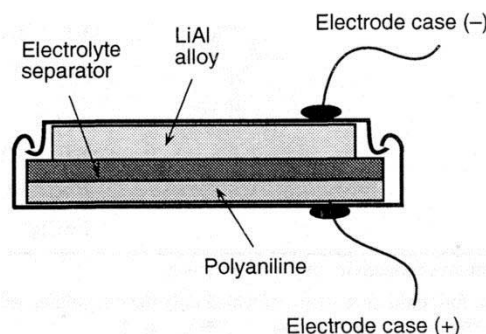


Figure 12-23 Illustration of a rechargeable battery using a polymeric cathode (polyaniline). The anode is a lithium–aluminum alloy, while the electrolyte can be a solution (e.g., propylene carbonate) of an appropriate salt or a solid polymer electrolyte (e.g., Li–PEO). Courtesy of M. G. Kanatzidis.

Other possible uses of conductive polymers include sensors, conductive paints, semiconductor circuits, low-current wires, electromechanical actuators, and photovoltaic (PV) material for use in solar cells as described in the following section. Applications of conductive polymers in photonic applications, including use in light-emitting diodes, as nonlinear optical material, variable-transmission (“smart”) windows, and electrochromic displays, are covered in Section 12.4.

12.3.3 Organic Photovoltaic Polymers

The potential of using light to produce electricity has been known since 1839 when Edmond Becquerel discovered that a current could be produced when a silver chloride electrode immersed in an electrolytic solution was connected to a counter metal electrode that was illuminated with white light. The current era in photovoltaic (PV) technology began in 1954 when scientists from Bell Laboratories [18] showed that *solar cells* based on *p-n* junctions in single crystals of silicon could be used to produce electricity. Efficiencies^{*} of these early inorganic photovoltaic (IPV) solar cells were in the range from 5% to 6%. Traditional applications included satellite power and roof-top power sources. Today, commercial Si-based solar cells can have overall power conversion efficiencies up to about 20%.

* Solar cell efficiency (%) = $\frac{\text{Power out (W)} \times 100\%}{\text{Area (m}^2\text{)} \times 1000 \text{ W/m}^2}$.

Another class of solar-cell materials, organic photovoltaics (OPV), includes photovoltaic polymers (PPVs). Polymeric solar cells (PSCs) provide several advantages over inorganic photovoltaic devices such as ease of fabrication using solution-based processing, low weight, and the flexibility to conform to the shape of a variety of supporting structures. Applications are diverse and include roof shingles, solar curtains, and even solar backpack chargers; however, current efficiencies of PSCs, with highest reported [19] efficiencies of around 10%, are currently much lower than those of Si-based solar cells (>20%).

The mechanisms of photoconversion also differ between IPV and OPV solar cells [20]. In the case of IPV solar cells, light absorption leads to the creation of *free* electron–“hole” pairs. In contrast, *excitons* [21] are formed in OPV solar cells. Excitons, electrically neutral quasiparticles, are mobile excited states consisting of a *bound* electron and a hole. The exciton radius is considered to be ~1 nm with binding energy ~0.4 to 1.0 eV. Excitons can transmit energy without transporting net charge. They can be dissociated at interfaces of materials with different electron affinities. Blending conjugated polymers with high-electron affinity molecules in bulk-heterojunction (BHJ) solar cells, illustrated in Figure 12-24, promotes rapid exciton dissociation.

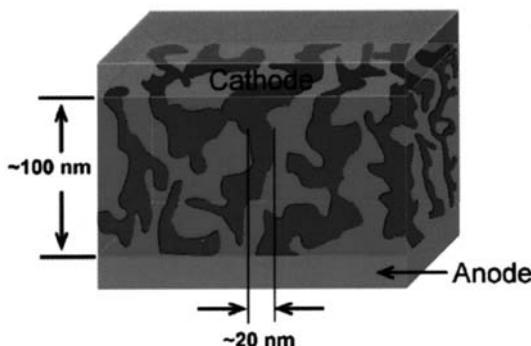
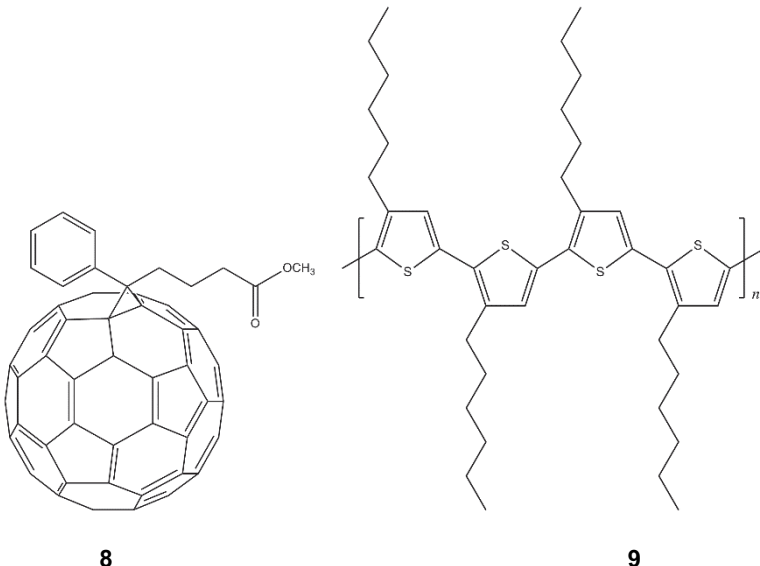


Figure 12-24 Illustration of a typical BHJ morphology showing acceptor–donor interfacial regions. Reproduced with permission from X. Yang and J. Loos, *Toward High Performance Polymer Solar Cells: The Importance of Morphology Control*. *Macromolecules*, 2007. **40**(5): p. 1353–1362, Copyright 2007 American Chemical Society.

Electron acceptors are typically a fullerene* or a chemically modified fullerene such as 1-(3-methoxy-carbonyl)propyl-1-phenyl-[6,6]-methanofullerene (PCBM). Donor polymers include those that have π -conjugation such as poly(3-hexylthio-

* Fullerenes are also called a buckminsterfullerene, buckyball, or simply C₆₀.

phene) (P3HT) and poly(1,4-phenylenevinylene) (PPV), poly[oxa-1,4-phenylene-(1-cyano-1,2-vinylene)-(2-methoxy-5-(3',7'-dimethyoctyloxy)-1,4-phenylene-1,2-(2-cyano-vinylene)-1,4-phenylene] (PCNEPV), and poly[2-methoxy-5-(3',7'-dimethyoctyl-oxy)-1,4-phenylenevinylene] (MDMO-PPV). At the molecular level, conjugated polymers such as P3HT become electron donors as electrons are promoted to the antibonding π^* band upon photoexcitation. Structures of PCBM, P3HT, PCNEPV, and MDMO-PPV, are shown in structures 8–11, respectively. A more detailed look at a representative BHJ solar cell using an MDMO-PPV electron donor and a PCBM electron-acceptor is illustrated in Figure 12-25. Important considerations for the design of high-efficiency BHJ solar cells include (a) a broad absorption range and strong absorption coefficient in the solar spectrum; (b) a bicontinuous network with domain width less than twice the exciton diffusion length; and (c) high donor-acceptor interfacial area to facilitate exciton dissociation and transport of separated charges to their respective electrodes [22].



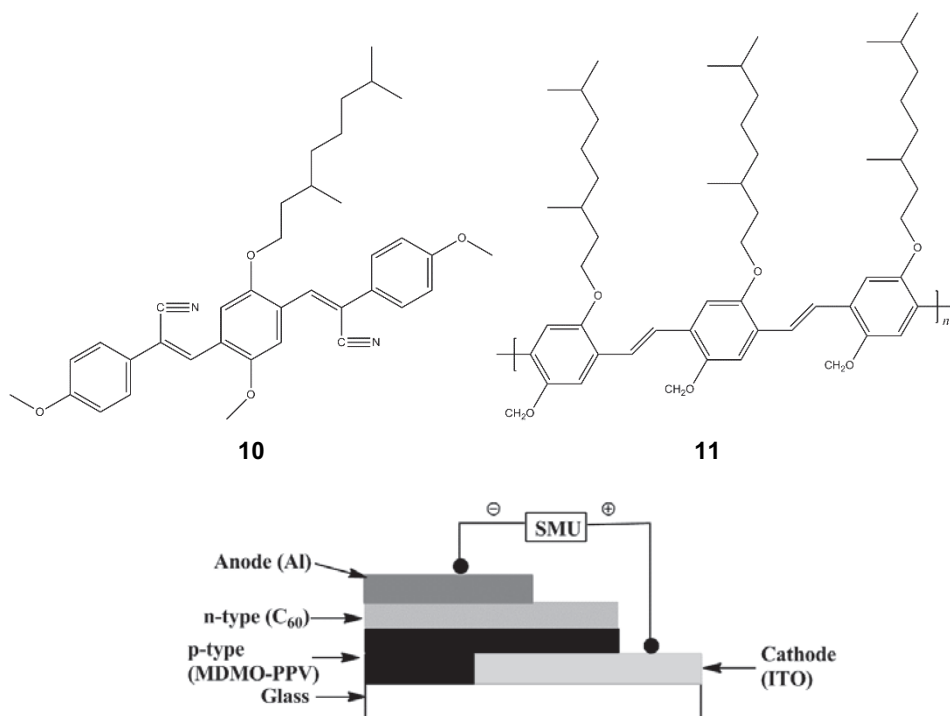


Figure 12-25 Detailed illustration of an MDMO-PPV/fullerene BHV. In this example, the cathode is a coating of indium tin oxide (ITO) on glass, the anode is aluminum, and SMU is an abbreviation for source measurement unit. Adapted from C. J. Brabec, N. S. Sariciftci, and J. C. Hummelen, *Plastic Solar Cells*. Advanced Functional Materials, 2001. 11(1): p. 15–26.

12.3.4 Electronic Shielding

Undesirable signals in the radio frequency (RF) range emitted by many electrical devices such as computers can interfere with normal RF reception. This behavior is called electromagnetic interference (EMI). Regulations from the Federal Communications Commission (FCC) have placed restrictions on RF transmissions by computers and other electrical devices. Unfilled polymers, typically insulating material, provide very little EMI shielding capability. There are two basic approaches that can be used to achieve EMI shielding for plastic enclosures. One includes coating the plastic with a conductive metal; the other involves blending the plastic with conductive fiber or particles. Generally, carbon- and metal-filled composites such as PVC filled with aluminum flakes provide suitable housings for low-emission electronic devices.

12.3.5 Dielectrics

A current challenge in materials science is the development of low-dielectric-constant or low- k materials to replace SiO₂. Silicon dioxide ($k = 4.2$) is an inadequate insulator to prevent “cross talk” between the closely spaced copper wire of the latest generation of semiconductors. For the 0.10-μm circuit lines required for the next-generation computer chips, k must be 2.5 or lower. Some polymers, particularly porous polymers, may be able to meet these needs with k values as low as 1.9. A variety of polymers have been proposed for low- k materials. These include polyimides, heteroaromatic polymers, poly(aryl ethers), and fluoropolymers. Polyimides, such as Kapton (see Section 10.2.1), had been used from the early 1970s to the late 1980s as inter-metal dielectrics. The dielectric constants of polytetrafluoroethylene and some of its derivatives (Section 10.1.9) are among the lowest of all polymers (between 1.9 and 2.1). In general, fluorine substitution decreases the dielectric constant of a polymer including polyimides. One of the biggest challenges may be thermal stability as the low- k polymers must be able to withstand temperatures of 400° to 450°C for several hours during annealing steps required to provide void-free copper deposits. Practically, this means that the thermal decomposition temperature must be far in excess of 500°C. Fabrication techniques include chemical vapor deposition (CVD), plasma-enhanced CVD, and spin coating.

12.3.6 Electronic Encapsulation

Polymers are used to provide integrated-circuit devices with a protective seal against moisture, radiation, and ion contamination. Thermosets, thermoplastics, and elastomers are all used as encapsulants. Included among thermosets are thermosetting polyimides, epoxies, unsaturated polyesters, and alkyd resins, as reviewed in Section 9.3. Candidates among thermoplastic encapsulants are poly(vinyl chloride), polystyrene, polyethylene, fluoropolymers, and acrylics. Elastomers can include silicone rubber and polyurethanes. For the most critical applications, epoxies and polyimides are favored.

12.4 Photonic Polymers

The next technological revolution may be the widespread use of optical rather than electronic devices for both storage and processing of data. Optical technology has the advantages of both speed and compactness of storage space. Optical storage of computer data is already common (i.e., CD-ROM and WORM drives) and ways to use optical devices for processing data are being explored. Among materials that are

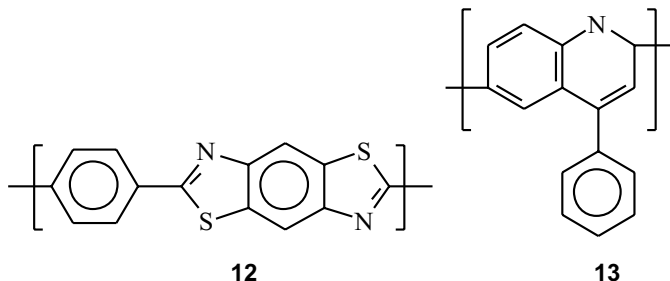
suitable for optical technology are polymers that exhibit *nonlinear optical* (NLO) properties. This means that their optical properties vary with the intensity of the light compared to ordinary glass, which is linear in its optical properties. Photore sponsive sunglasses that change tint with the intensity of sunlight are examples of NLO materials.

12.4.1 Nonlinear Optical Polymers

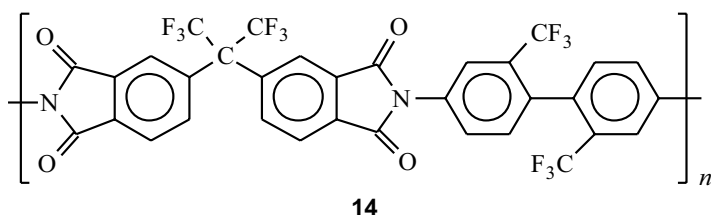
Unlike other materials, the refractive index of a nonlinear optical (NLO) material is not constant but a function of the intensity of the incident light striking it. For NLO effects to be observed, the light must be coherent and intense such as is produced by a laser. NLO behavior can be first-order or second-order depending upon whether nonlinear effects are dependent upon the first-order hyperpolarizability tensor term, $\chi^{(2)}$, or the second-order hyperpolarizability term, $\chi^{(3)}$, in the equation for the polarizability (P) of the bulk material

$$P = \chi^{(1)}E + \chi^{(2)}E \cdot E + \chi^{(3)}E \cdot E \cdot E + \dots \quad (12.26)$$

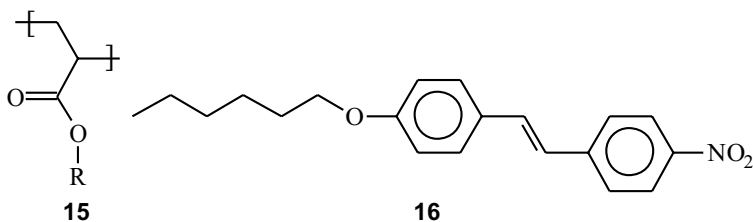
where E is the external electric field. Third-order nonlinear materials are important for optical signal processing. Materials that have significant third-order NLO behavior have a small optical band gap, high concentration of easily polarizable electrons, and a large effective conjugation length. Polymers that exhibit third-order nonlinearity include many of the conductive polymers listed in Table 12-11 such as polyacetylene, poly(*p*-phenylene vinylene) (PPV), polythiophene (PT), and polyaniline (PANI). Others include poly(*p*-phenylene benzo-bisthiazole) (PBZT, structure 12) and polyquinoline (PPQ, structure 13). Other possibilities include modified rigid-rod polyimides with NLO-active side groups.



In general, molecules with π -electron structures can exhibit NLO effects when these electrons are optically excited. In the case of polymers, these π -electron structures can be part of the main-chain backbone, as for example in the case of the 6F-polyimide (structure 14, see Section 10.2.1).



The NLO functionality can also be incorporated as a side chain, as in the case of an acrylate polymer (structure 15) having a substituent group (R) that contains a 4-methoxy-4'-nitrostilbene moiety connected by a six-carbon spacer (structure 16)



12.4.2 Light-Emitting Diodes

A light-emitting diode (LED) is a crystalline semiconductor chip that glows. Only red and green were available colors for the first LEDs introduced in the 1960s. An organic light-emitting diode, or OLED, is made of sheets of polymer semiconductor material resembling plastic, as shown in Figure 12-26. Polymer LEDs were discovered by Richard Friend and coworkers at Cambridge University in 1989 and now provide a full palette of light. The first polymer exhibiting light emission, green-yellow in color, was PPV (see Table 12-11), which had low efficiency and short lifetime. Substitution of the phenylene ring of PPV with alkoxy groups (structure 17) such as illustrated below results in emission in the orange-red range while poly(*p*-phenylene) emits blue light. LEDs can provide light at very high efficiency (up to 75% of electric consumption can be converted to light). Polymers like the substituted polythiophene, poly[3-(4-octylphenyl)-2,2'-bithiophene] (structure 18), will luminesce with polarized light when an electric current is passed through them. A variety of polymer configurations including block copolymers, side-chain polymers, and even dendrimers (see Section 10.2.9) provide opportunities for LEDs.

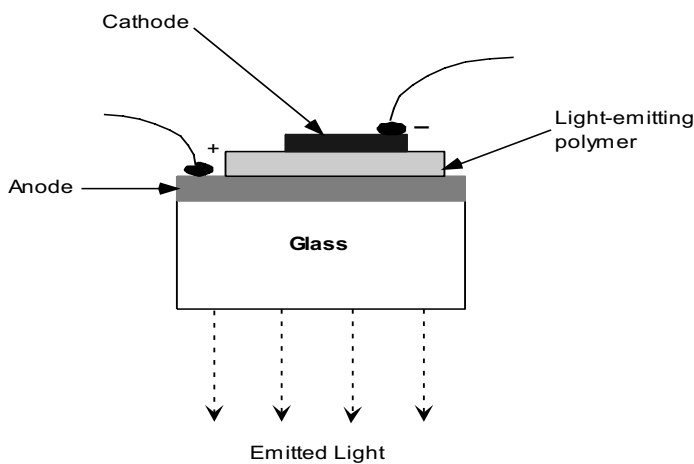
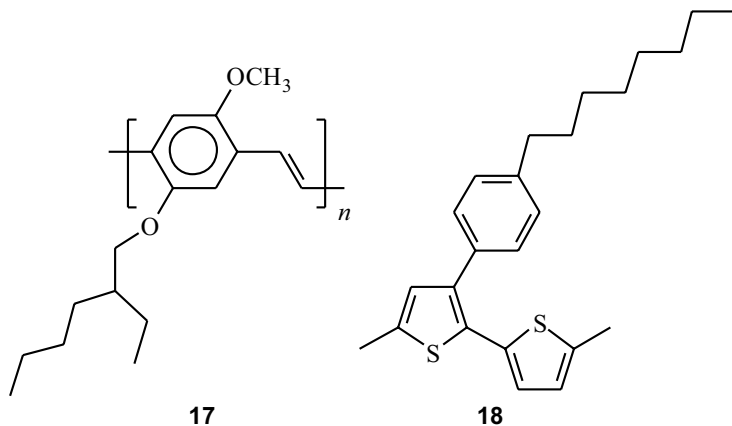


Figure 12-26 Basic design of a polymer LED.



12.5 Sensor Applications

Polymers have been used to replace other materials such as inorganic semiconductors, metals, catalysts, and solid electrolytes in a variety of sensing devices [23–25]. These include many diverse applications such as pH measurements, gas sensing, explosives detection, humidity measurements, and biosensing. In many of these cases, the physical or electrical response of semiconducting polymers to a specific molecule, the *analyte*, provides the basis for sensing.

In the design of chemical sensors, a receptor site that provides some form of molecular recognition for a given analyte is connected to a signaling unit. The binding event results in a property change that can be measured. The chemosensor can be modified by changing its binding constant and selectivity and through modification of the transduction efficiency between the binding event and the resulting signal. The signal can be electrical resulting from changes in capacitance or resistance or optical through changes in fluorescence or absorption. Two related approaches to forming a generic chemical sensor from a thiophene polymer structure are illustrated in Figure 12-27. A specific crown ether receptor that can be used for sodium cation detection is illustrated in Figure 12-28. Conformation twisting of the polythiophene can result in a drop in conductivity of 10^5 or more.

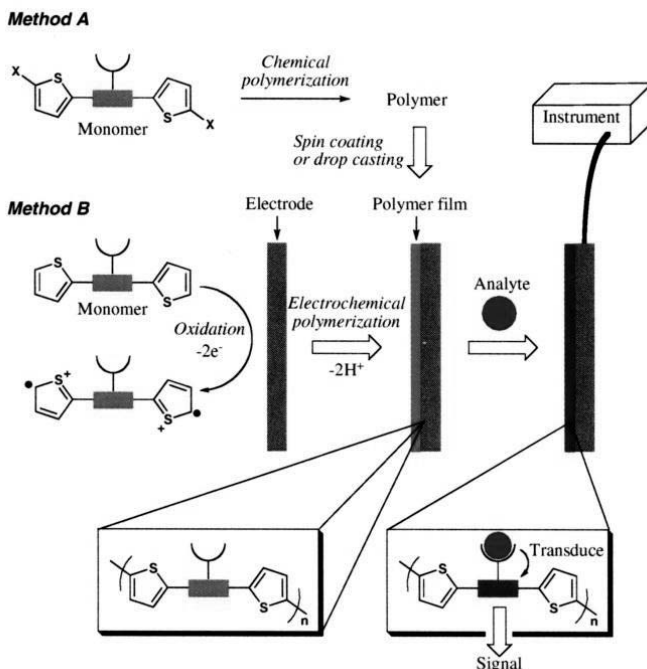


Figure 12-27 Illustration of two related approaches to developing a chemical sensor using a semiconducting polymer containing receptor sites. In Method A, a thiophene derivative is spin-coated or drop-coated on a suitable electrode. In Method B, the monomer is polymerized on the electrode using anodic electrochemical polymerization. Reproduced from K. Sugiyasu and T. M. Swager, *Conducting Polymer-Based Chemical Sensors: Transduction Mechanisms*. Bulletin of the Chemical Society of Japan, 2007. **80**(11): p. 2074–2083.

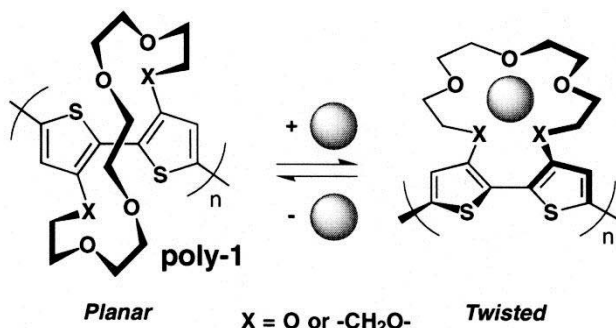
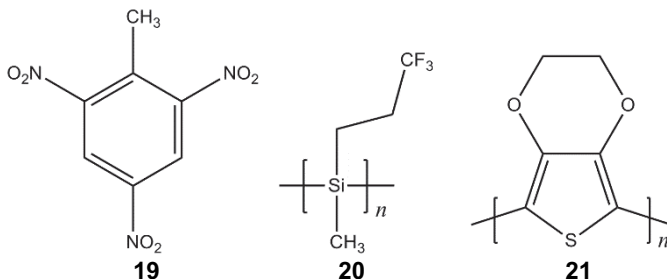


Figure 12-28 Conformation changes induced upon the insertion of an alkali metal cation inside a crown-ether-modified polythiophene. Reproduced from K. Sugiyasu and T. M. Swager, *Conducting Polymer-Based Chemical Sensors: Transduction Mechanisms*. Bulletin of the Chemical Society of Japan, 2007. **80**(11): p. 2074-2083.

Explosives Detection. An important application of chemical sensors is the detection of nitroaromatic explosives [26], especially trinitrotoluene (TNT, structure 19), which is an ingredient of many explosives and also poses environmental health risks. Nitroaromatics are electron accepting while conjugated polymers are electron donors. On this basis, nitroaromatic analytes can act as electron acceptors for photoexcited electrons of conjugated polymers including substituted polyacetylenes, poly(*p*-phenylenevinylenes), poly(*p*-phenyleneethynylenes), and polymeric porphyrins. In the presence of nitroaromatics, polymers such as poly(3,3,3-trifluoropropylmethylsilane) (PTFPMS, structure 20) exhibit photoluminescence quenching that provides another means for detection.

Gas Sensors. Conjugated polymers such as polyaniline, polypyrrole, and poly(3,4-ethylenedioxythiophene) (PEDOT, structure 121) also can be used in sensing devices for gases such as CO, H₂, NH₃ (an electron donor), and NO₂ (an electron acceptor) as well as airborne organic vapors such as halocarbons, alcohols, and ethers [27].



SUGGESTED READING

MEMBRANES

- Baker, R. W., J. G. Wijmans, and J. H. Kaschekat, *The Design of Membrane Vapor–Gas Separation Systems*. Journal of Membrane Science, 1998. **151**: p. 55.
- Belfort, G., *Synthetic Membrane Processes*. 1984, Orlando: Academic Press.
- Brüschke, H., *Industrial Application of Membrane Separation Processes*. Pure and Applied Chemistry, 1995. **67**: p. 993.
- Comyn, J., *Polymer Permeability*. 1985, London: Elsevier Applied Science Publishers.
- Crank, J., *The Mathematics of Diffusion*. 1975, New York: Oxford University Press.
- Crank, J., and G. S. Park, *Diffusion in Polymers*. 1968, London: Academic Press.
- Feldman, D., *Polymer Barrier Films*. Journal of Polymers and the Environment, 2002. **9**: p. 49.
- Feng, X., and R. Y. M. Huang, *Liquid Separation by Membrane Pervaporation: A Review*. Industrial and Engineering Chemistry and Research, 1997. **36**: p. 1048.
- Gilron, J., and A. Soffer, *Knudsen Diffusion in Microporous Carbon Membranes with Molecular Sieving Character*. Journal of Membrane Science, 2002. **209**: p. 339.
- Henis, J. M. S., and M. K. Tripodi, *The Developing Technology of Gas Separating Membranes*. Science, 1983. **220**: p. 11.
- Ho, W. S., and K. K. Sirkar, eds., *Membrane Handbook*. 1992, New York: Van Nostrand Reinhold.
- Huang, R. Y. M., *Pervaporation Membrane Separation Processes*. 1991, Amsterdam: Elsevier.
- Kesting, R. E., *Synthetic Polymeric Membranes*. 1985, New York: John Wiley & Sons.
- Kesting, R. E., and A. K. Fritzsche, *Polymeric Gas Separation Membranes*. 1993, New York: John Wiley & Sons.
- Koros, W. J., ed., *Barrier Polymers and Structures*. ACS Symposium Series 423. 1990, Washington, DC: American Chemical Society.
- Koros, W. J., and G. K. Fleming, *Membrane-Based Gas Separation*. Journal of Membrane Science, 1993. **83**: p. 1.
- Koros, W. J., *Membranes: Learning a Lesson from Nature*. Chemical Engineering Progress. October 1995, p. 68.
- Matsuura, T., *Synthetic Membranes and Membrane Separation Processes*. 1994, Boca Raton: CRC Press.
- Mulder, M., *Basic Principles of Membrane Technology*. 1991, Dordrecht: Kluwer Academic Publishers.
- Park, J. H., S. Lee, J.-H. Kim, K. Park, K. Kim, and I. C. Kwon, *Polymeric Nanomedicine for Cancer Therapy*. Progress in Polymer Science, 2008. **33**: p. 113.
- Paul, D. R., *Gas Sorption and Transport in Glassy Polymers*. Berichte der Bunsengesellschaft für Physikalische Chemie, 1979. **83**: p. 294.

- Phair, J. W., and S. P. S. Badwal, *Materials for Separation Membranes in Hydrogen and Oxygen Production and Future Power Generation*. Science and Technology of Advanced Materials Science, 2006. **M7**: p. 792–805.
- Strathmann, H., *Membrane Separation Processes: Current Relevance and Future Opportunities*. AIChE Journal, 2001. **47**: p. 1077.
- Wynn, N., *Pervaporation Comes of Age*. Chemical Engineering Progress. October 2001, p. 66–72.

BIOMEDICAL APPLICATIONS

- Bajpai, A. K., S. K. Shukla, S. Nhanu, and S. Kankane, *Responsive Polymers in Controlled Drug Delivery*. Progress in Polymer Science, 2008. **33**: p. 1088.
- Dash, M., F. Chiellini, R. M. Ottenbrite, and E. Chiellini, *Chitosan—a Versatile Semi-Synthetic Polymer in Biomedical Applications*. Progress in Polymer Science, 2011. **36**: p. 981.
- De Bartolo, L., S. Morelli, A. Bader, and E. Drioli, *Evaluation of Cell Behaviour Related to Physico-Chemical Properties of Polymeric Membranes to Be Used in Bioartificial Organs*. Biomaterials, 2002. **23**: p. 2485.
- Graham, N. B., and D. A. Wood, *Hydrogels and the Biodegradable Polymers for the Controlled Delivery of Drugs*. Polymer News, 1982. **8**: p. 230.
- Jagur-Grodzinski, J., *Biomedical Application of Functional Polymers*. Reactive and Functional Polymers, 1999. **39**: p. 99.
- Jagur-Grodzinski, J., *Polymers for Targeted and/or Sustained Drug Delivery*. Polymers for Advanced Technologies, 2009. **20**: p. 595.
- Jeong, J. H., *Molecular Design of Functional Polymers for Gene Therapy*. Progress in Polymer Science, 2007. **32**: p. 1239.
- Kenawy, E.-R., S. D. Worley, and R. Broughton, *The Chemistry and Applications of Antimicrobial Polymers: A State-of-the Art Review*. Biomacromolecules, 2007. **8**(5): p. 1360.
- Khandare, J., and T. Minko, *Polymer–Drug Conjugates: Progress in Polymeric Prodrugs*. Progress in Polymer Science, 2006. **31**: p. 359.
- Kost, J., *Hydrogels for Controlled Delivery of Bioactive Agents*. Polymer News, 1995. **20**: p. 73.
- Langer, R., and N. A. Peppas, *Advances in Biomaterials, Drug Delivery, and Bionanotechnology*. AIChE Journal, 2003. **49**(12): p. 2990.
- Langer, R., and J. P. Vacanti, *Tissue Engineering*. Science, 1993. **260**: p. 920.
- Martina, M., and D. W. Hutmacher, *Biodegradable Polymers Applied in Tissue Engineering Research: A Review*. Polymer International, 2007. **56**: p. 145.
- Mulligan, R. C., *The Basic Science of Gene Therapy*. Science, 1993. **260**: p. 926.
- Ottenbrite, R. M., ed., *Polymeric Drugs and Drug Administration*. ACS Symposium Series 545. 1994, Washington, DC: American Chemical Society.
- Pack, D. W., A. S. Hoffman, S. Pun, and P. S. Stayton, *Design and Development of Polymers for Gene Delivery*. Nature Reviews: Drug Discovery, 2005. **4**: p. 581.
- Park, J. H., S. Lee, J.-H. Kim, K. Park, K. Kim, and I. C. Kwon, *Polymeric Nanomedicine for Cancer Therapy*. Progress in Polymer Science, 2008. **33**: p. 113.

- Schaffert, D., and E. Wagner, *Gene Therapy Progress and Prospects: Synthetic Polymer-Based Systems*. Gene Therapy, 2008. **15**: p. 1131.
- Stamatialis, D. F., B. J. Papenburg, M. Girones, S. Saiful, S. N. M. Bettahalli, S. Schmitmeyer, and M. Wessling, *Medical Applications of Membranes: Drug Delivery, Artificial Organs, and Tissue Engineering*. Journal of Membrane Science, 2008. **308**: p. 1.
- Sugibayashi, K., and Y. Morimoto, *Polymers for Transdermal Drug Delivery Systems*. Journal of Controlled Release, 1994. **29**: p. 177.
- Suzuki, M., and O. Hirasa, *An Approach to Artificial Muscle Using Polymer Gels Formed by Micro-Phase Separation*. Advances in Polymer Science, 1993. **110**: p. 241.
- Wong, S. Y., J. M. Pelet, and D. Putman, *Polymer Systems for Gene Delivery—Past, Present, and Future*. Progress in Polymer Science, 2007. **32**: p. 799.

ELECTRONICS AND ENERGY

- Goetzberger, A., C. Hebling, and H.-W. Schock, *Photovoltaic Materials, History, Status, and Outlook*. Materials Science and Engineering, 2003. **40**: p. 1.
- Hadzioannou, G., and G. G. Malliaras, eds., *Semiconducting Polymers: Chemistry, Physics and Engineering*. 2007, Weinheim: Wiley-VCH.
- Heeger, A. J., *Charge Storage in Conducting Polymers: Solitons, Polarons, and Bipolarons*. Polymer Journal, 1985. **17**: p. 201.
- Heeger, A. J., *Semiconducting and Metallic Polymers: The Fourth Generation of Polymeric Materials*. Synthetic Metals, 2002. **125**: p. 23.
- Hoppe, H., and N. S. Sariciftci, *Organic Solar Cells: An Overview*. Journal of Materials Research, 2004 **19**(7): p. 1924.
- Huang, J.-C., *EMI Shielding Plastics: A Review*. Advanced Polymer Technology, 1995. **14**: p. 137.
- Kaner, R. B., and A. G. MacDiarmid, *Plastics That Conduct Electricity*. Scientific American, February 1988, p. 106.
- Ku, C. C., and R. Liepins, *Electrical Properties of Polymers*. 1987, Munich: Hanser Publications.
- MacDiarmid, A. G., *Synthetic Metals: A Novel Role for Organic Polymers*. Synthetic Metals, 2002. **125**: p. 11.
- Margolis, J. M., ed., *Conductive Polymers and Plastics*. 1989, New York: Chapman and Hall.
- Patel, J. S., *Liquid Crystal: Materials for Displays*. Annual Review of Materials Science. **23**: p. 269.

PHOTONICS

- Jacobson, S., P. Landi, T. Findakly, J. Stamatoff, and H. Yoon, *Nonlinear Optical Polymers in Advanced Photonics*. Journal of Applied Polymer Science, 1994. **53**: p. 649.
- Lee, K.-S., ed., *Polymers for Photonics Applications I*. Advances in Polymer Science 158. 2002, Berlin: Springer-Verlag.
- Reinhardt, B. A., *The Status of Third-Order Polymeric Nonlinear Optical Materials: Directions and Philosophy of Polymer Research for Nonlinear Optics in the U.S. Air Force Wright Laboratory*. Trends in Polymer Science, January 1993, p. 4.

PROBLEMS

12.1 An asymmetric hollow fiber of polysulfone has a surface pore area, A_3/A_2 , of 1.9×10^{-6} and an effective skin thickness of 1000 \AA . If the fiber is coated with a $1\text{-}\mu\text{m}$ layer of silicone rubber, calculate the effective P/ℓ for the coated membrane for CO_2 and the perm-selectivity for CO_2/CH_4 .

12.2 What pore size is required for Knudsen flow of oxygen and nitrogen through a porous membrane? What would be the ratio of diffusion coefficient, $D(\text{O}_2)/D(\text{N}_2)$, for the permeation of air through this membrane? How does this ratio compare to that for the permeation of air through a polysulfone hollow-fiber membrane? How does this ratio of diffusion coefficients compare to the ideal permselectivity, $\alpha(\text{O}_2, \text{N}_2)$, reported for oxygen/nitrogen through the polysulfone membrane?

12.3 What are the limitations, if any, to the statement that $P = SD$ (eq. (12.7))?

12.4 What are the principal applications of pervaporation in the chemical industry? For these cases, how do the economics of pervaporation compare with more traditional separation methods in the United States and in Europe?

12.5 What are the principal applications for polymeric fuel-cell membranes? What are their advantages and limitations compared to other proton-conduction membranes?

12.6 For encapsulation of islet cells for medical implants in humans, what polymers would be most suitable? Discuss your choices.

REFERENCES

1. Salame, M., *Transport Properties of Nitrile Polymers*. Journal of Polymer Science, Polymer Symposium, 1973. **41**: p. 1–15.
2. Salame, M., *Prediction of Gas Barrier Properties of High Polymers*. Polymer Engineering and Science, 1986. **26**(22): p. 1543–1546.
3. Nagai, K., et al., *Poly[1-(trimethylsilyl)-1-propyne] and Related Polymers: Synthesis, Properties, and Functions*. Progress in Polymer Science, 2001. **26**: p. 721–798.
4. Robeson, L. M., *The Upper Bound Revisited*. Journal of Membrane Science, 2008. **320**: p. 390–400.
5. Heinzel, A., and V. M. Barragan, *A Review of the State-of-the-Art of the Methanol Crossover in Direct Methanol Fuel Cells*. Journal of Power Sources, 1999. **84**: p. 70–74.
6. Vieth, W. R., J. M. Howell, and J. H. Hsieh, *Dual Sorption Theory*. Journal of Membrane Science, 1976. **1**: p. 177–220.
7. Teplyakov, V., and P. Meares, *Correlation Aspects of the Selective Gas Permeabilities of Polymeric Materials and Membranes*. Gas Separation and Purification, 1990. **4**: p. 66–74.
8. Paul, D. R., and W. J. Koros, *Effect of Partially Immobilizing Sorption on Permeability and the Diffusion Time Lag*. Journal of Polymer Science: Polymer Physics Edition, 1976. **14**: p. 675–685.

9. Gierke, T. D., and W. Y. Hsu, *The Cluster-Network Model of Ion Clustering in Perfluorinated Membranes*, in *ACS Symposium Series*, A. Eisenberg and H. L. Yeager, eds. 1982, Washington DC: American Chemical Society, p. 283–307.
10. Loeb, S., and S. Sourirajan, *Sea Water Determination by Means of a Semiempirical Membrane*. University of California, Los Angeles, Report No. 60-60, 1960.
11. Henis, J. M. S., and M. K. Tripodi, *Composite Hollow Fiber Membranes for Gas Separation: The Resistance Model Approach*. *Journal of Membrane Science*, 1981. **8**(3): p. 233–246.
12. Park, J. H., et al., *Polymeric Nanomedicine for Cancer Therapy*. *Progress in Polymer Science*, 2008. **33**: p. 113–137.
13. Pack, D. W., et al., *Design and Development of Polymers for Gene Delivery*. *Nature Reviews: Drug Discovery*, 2005. **4**: p. 581–593.
14. Kenaway, E.-R., S. D. Worley, and R. Broughton, *The Chemistry and Applications of Antimicrobial Polymers: A State-of-the-Art Review*. *Biomacromolecules*, 2007. **8**(5): p. 1359–1384.
15. Martino, A. D., M. Sittoner, and M. V. Risbud, *Chitosan: A Versatile Biopolymer for Orthopaedic Tissue-Engineering*. *Biomaterials*, 2005. **26**: p. 5983–5990.
16. Shoichet, M. S., *Polymer Scaffolds for Biomaterials Applications*. *Macromolecules*, 2010. **43**: p. 581–591.
17. Martina, M., and D. W. Hutmacher, *Biodegradable Polymers Applied in Tissue Engineering Research: A Review*. *Polymer International*, 2007. **56**: p. 145–157.
18. Chapin, D. M., C. S. Fuller, and G. L. Pearson, *A New p-n Junction Photocell for Converting Solar Radiation into Electrical Power*. *Journal of Applied Physics*, 2012. **25**: p. 676–677.
19. Chen, H.-Y., et al., *Polymer Solar Cells with Enhanced Open-Circuit Voltage and Efficiency*. *Nature Photonics*, 2009. **3**: p. 649–653.
20. Gregg, B. A., and M. C. Hanna, *Comparing Organic to Inorganic Photovoltaic Cells: Theory, Experiment, and Simulation*. *Journal of Applied Physics*, 2003. **93**(6): p. 3505–3614.
21. Liang, W. Y., *Excitons*. *Physics Education*, 1970. **5**(4): p. 226–228.
22. Liang, Y., and L. Yu, *A New Class of Semiconducting Polymers for Bulk Heterojunction Solar Cells with Exceptionally High Performance*. *Accounts of Chemical Research*, 2010. **43**(9): p. 1227–1236.
23. Dai, L., P. Soundarajan, and T. Kim, *Sensors and Sensor Arrays Based on Conjugated Polymers and Carbon Nanotubes*. *Pure and Applied Chemistry*, 2002. **74**(9): p. 1753–1772.
24. Adhikari, B., and S. Majumdar, *Polymers in Sensor Applications*. *Progress in Polymer Science*, 2004. **29**: p. 699–766.
25. Lange, U., N. V. Roznyatovskaya, and V. M. Mirsky, *Conducting Polymers in Chemical Sensors and Arrays*. *Analytica Chimica Acta*, 2008. **614**: p. 1–26.
26. Toal, S. J., and W. C. Trogler, *Polymer Sensors for Nitroaromatic Explosives Detection*. *Journal of Materials and Chemistry*, 2006. **16**: p. 2871–2883.
27. Bai, H., and G. Shi, *Gas Sensors Based on Conducting Polymers*. *Sensors*, 2007. **7**: p. 267–307.

This page intentionally left blank